Can the combining of wetlands with reservoir operation reduce the risk of future flood and droughts?

Yanfeng Wu[1], Jingxuan Sun[1,2], Boting Hu[1,2], Y. Jun Xu[3], Alain N. Rousseau[4], Guangxin Zhang[1,*]

[1] Northeast Institute of Geography and Agroecology, Chinese Academy of Sciences, Changchun, Jilin 130102, China

[2] University of Chinese Academy of Sciences, Beijing 100049, China

[3] School of Renewable Natural Resources, Louisiana State University Agricultural Center, 227 Highland Road, Baton Rouge, LA 70803, USA

[4] INRS-ETE / Institut National de la Recherche Scientifique - Eau Terre Environnement, 490 rue de la Couronne, G1K 9A9 Quebec City, Quebec, Canada

* Correspondence: Professor Guangxin Zhang (zhgx@iga.ac.cn)

Abstract. Wetlands and reservoirs are important water flow and storage regulators in a river basin; therefore, they can play a crucial role in mitigating flood and hydrological drought risks. Despite the advancement of river basin theory and modeling, our knowledge is still limited about the extent that these two regulators could have in performing such a role, especially under future climate extremes. To improve our understanding, we first coupled wetlands and reservoir operations into a semi-spatially explicit hydrological model and then applied it in a case study involving a large river basin in Northeast China. The projection of future floods and hydrological droughts was performed using the hydrological model during different periods (near-future: 2026-2050, mid-century: 2051-2075, and end-century: 2076-2100) under five future climate change scenarios. We found that the risk of future floods and hydrological droughts can vary across different periods, in particular, will experience relatively large increases and slight decreases. This large river basin will experience longer duration, larger peak flows and volume, and enhanced flashiness flood events than the historical period. Simultaneously, the hydrological droughts will be much more frequent with longer duration and more serious deficit. Therefore, the risk of floods and droughts will overall increase further under future climate change even under the combined influence of reservoirs and wetlands. These findings highlight the hydrological

28   regulation function of wetlands and reservoirs and attest that the combining of wetlands with reservoir

29   operation cannot fully eliminate the increasing future flood and drought risks. To improve a river basin's

30   resilience to the risks of future climate change, we argue that implementation of wetland restoration and

31   development of accurate forecasting systems for effective reservoir operation are of great importance.

32   Furthermore, this study demonstrated a wetland-reservoir integrated modeling and assessment

33   framework that is conducive to risk assessment of floods and hydrological droughts, which can be used

34   for other river basins in the world.

35   **Keywords**: Climate change; Hydrologic projection; Floods and droughts; Wetland hydrological

36   services; Reservoir operations; Model integration

37

38   **1. Introduction**

39   Floods and droughts have produced some of the most frequent and serious disasters in the world

40   (Diffenbaugh et al., 2015; Hirabayashi et al., 2013; UNISDR, 2015). Globally, they account for 38% of

41   the total number of natural disasters, 45% of the total casualties, more than 84% of the total number of

42   people affected, and 30% of the total economic damage caused by all-natural disasters (Güneralp et al.,

43   2015) in the past. As climate change has been accelerating the hydrological cycle, causing more frequent

44   and stronger weather extremes, more floods and droughts have been projected to increase at both global

45   (Chiang et al., 2021; Jongman, 2018) and regional scales (Hallegatte et al., 2013; Wang et al., 2021).

46   Concurrently, the disaster-related loss of ecosystems (e.g., wetlands, forest, and grassland) and their

47   services can mitigate the flood and drought risks to a great extent (Gulbin et al., 2019; Walz et al., 2021).

48   Given this, grey infrastructure such as dams, dikes, and reservoirs, which have often been used to

49   attenuate flood and drought hazards because of their rapid and visible effects, can play an important role

50   in ensuring the water security of a river basin (Alves et al., 2019; Casal-Campos et al., 2015). However,

51   relying solely on grey infrastructure to attenuate floods and droughts has some inadequacies, such as

52   large investments to build and maintain in addition to adverse effects on downstream ecosystems (Maes

53   et al., 2015; Schneider et al., 2017). In this context, Nature-based solutions (NBS) for hydro-

meteorological hazards mitigation are becoming increasingly popular (Kumar et al., 2021), because

NBS can effectively reduce or even offset the hydrological processes driving floods and droughts (Nika

et al., 2020), while making least disturbance to the environment as well as delivering co-benefits which

grey infrastructure cannot provide (Anderson and Renaud, 2021; Nelson et al., 2020). Therefore, it is

urgent to integrate NBS into the current water management practices to increase basin resilience to

hydrological extremes under climate change.

Wetlands have the potential to be used as a NBS for improving water storage and hence the resilience

of a river basin to hydrological extremes along with grey infrastructures (Thorslund et al., 2017). This

is because, similar to man-made dams and reservoirs, wetlands can attenuate flow and alter basin

hydrological processes (Lee et al., 2018), such as floods (Wu et al., 2020a) and baseflows (Evenson et

al., 2015; Wu et al., 2020b). However, unlike man-made grey infrastructures, wetlands are integral in

landscapes and they are connected laterally and vertically with the surrounding terrestrial and aquatic

environments through the hydrological cycling of water and waterborne substances (Ahlén et al., 2020),

making their water storage and cycling fundamental to estimate a watershed's water balance (Golden et

al., 2021; Shook et al., 2021). To understand how and to what extent wetlands can mitigate hydrological

processes, two approaches are commonly used: (i) description of individual wetland services at the field

scale (e.g., Park et al., 2014) or wetlandscape scale (e.g., Åhlén et al., 2022); (ii) assessment of wetland

hydrological services at the regional/watershed scale (Fossey et al., 2016; Wu et al., 2020a, 2020b).

However, the former approach can only be achieved with field observation with instruments and is

mainly used to provide key parameters of wetland processes for model calibration (Fossey and Rousseau,

2016). Recently, several wetland modules have been development and coupled to hydrological (e.g.,

Soil and Water Assessment Model, HYDROTEL model) to quantify hydrological function of wetlands,

particularly the mitigation services on floods and droughts (Evenson et al., 2018; Evenson et al., 2016;

Fossey et al., 2015a; Zeng et al., 2020). These wetland hydrological models not only consider the general

water budget of a river basin but also consider the perennial and intermittent hydrological interactions

between wetlands-to-wetlands and wetlands-to- surrounding landscapes. It is of both scientific and

practical interest to project wetland capability in mitigating floods and droughts in response to a

81   changing climate.

82   Reservoirs redistribute large amounts of surface water, thus altering natural hydrological processes,

83   such as flow range, flood and drought patterns, and basin water balances (Boulange et al., 2021; Chen

84   et al., 2021; Manfreda et al., 2021; Zhao et al., 2016). So far, throughout the world, there are 57, 985

85   reservoirs registered by the International Commission on Large Dams and their total volume has been

86   reached 14, 602 km^3 (Eriyagama et al., 2020). Such numerous reservoirs and their large storage capacity

87   should not be neglected in water hazard assessment and hydrological projection because of their

88   significant modification on flood and drought patterns (Boulange et al., 2021; Brunner et al., 2021). For

89   that reason, scholars called for the need to integrate reservoirs in model-based impact analysis of flood

90   exposure under climate change (Dang et al., 2020a; Yassin et al., 2019). Therefore, there is a growing

91   need in incorporating reservoir operations into basin hydrologic simulations and predictions.

92   Despite the well-established knowledge of flow regulation and water storage functions that wetlands

93   and reservoirs can provide in a river basin, most modeling assessments on floods and droughts at the

94   basin scale do not take the two components into account, or give little emphasis on the combined benefits

95   of them (Brunner et al., 2021; Golden et al., 2021). Nor are the hydrological processes associated with

96   these features implicitly included in the calibration of hydrologic models. Recent studies have suggested

97   that disregarding of the wetlands or reservoir operation would add significant error and larger

98   uncertainties to simulate hydrologic processes (Brunner et al., 2021; Ward et al., 2020). Because

99   wetlands are often abundant across many landscapes, which make their water storage and cycling

100 fundamental to estimate a watershed's water balance (Rains et al., 2016; Lee et al., 2018). Therefore,

101 missing this component of water balances could potentially lead to disproportionately large model errors

102 (Rajib et al., 2020). Consequently, integrating the wetlands (Fossey et al., 2015a; Golden et al., 2021;

103 Rajib et al., 2020) or reservoir operation (Dang et al., 2020; Yassin et al., 2019; Zhao et al., 2016) alone

104 into watershed-scale hydrologic models may largely minimize uncertainties and improve model

105 performance. Furthermore, on a global scale, most river basins have wetlands and their river flow has

106 or will experience reservoir regulation (Muller, 2019; Schneider et al., 2017), which elicits thought-

107 provoking concerns: What will be the changes of future floods and droughts under the combined

4

108   influence of wetlands and reservoirs? Such concern is important because the omission of wetlands and

109   reservoirs can cause the policy-making process to be imprecise at best and ineffective at worst. However,

110   a reservoir operation and wetland services, integrated basin-scale model rarely exist in the literature.

111   Furthermore, although few studies (e.g., Rajib et al. (2020; Chen et al., 2021; Wu et al., 2021) provide

112   insights into modeling and understanding the flow regulation functions provided by wetlands and

113   reservoirs, however, is it still unclear whether the combining of wetlands with reservoir operation can

114   largely reduce the risk of future floods and droughts.

115   Considering the above-introduced scientific challenges and management deficiencies, we first

116   developed a framework of hydrological modeling coupled with wetland modules and reservoir operation

117   scenarios. We then applied it to a large river basin with abundant wetlands and a large reservoir, the

118   Nenjiang River Basin in northeast China, to address a central question: Can the combining of wetlands

119   with reservoir operation largely reduce the risk of future flood and droughts? The Nejinang River Basin

120   was selected as a case study here because it has abundant wetlands and a large reservoir, and has

121   undergone intensive anthropogenic activities in the past half century, particularly in the increasing

122   agricultural water consumption and conversion of wetlands to agricultural and other land uses. Our

123   framework and results are expected to bring new insights into future floods and droughts and provide a

124   basis for decision-making to curb the growing impacts of unprecedented and future hydrological

125   extreme conditions.

126   **2. Methodology**

127   2.1 Study area and datasets

128   We conducted this analysis in the Nenjiang River Basin (NRB), a large river basin (291,700 km^2)

129   located in the Northeast China (Fig. 1). Long-term annual average runoff depth and volume from the

130   NRB are 97.4 mm and 22.7 billion m^3. The river basin is located in the middle-high latitudes and can

131   be characterized by a temperate semi-humid continental monsoon climate. Inter-annual differences in

132   temperature and precipitation are large, i.e., disparate hot and cold periods, and uneven dry and wet

133   conditions (Meng et al., 2019). The average annual temperature across the basin ranges between 2.1-

134 4.5°C. The annual total precipitation within the basin fluctuates from 323.1 to 537.6 mm. Precipitation

135 is mainly concentrated during June-September, which accounts for about 85% of the annual

136 precipitation (Li et al., 2014).

137 The NRB is one of the pivotal wetland areas in China. The basin contains several important wetland

138 conservation areas, among which Zhalong and Nanweng River Wetlands have been designated as a

139 Ramsar Site of International Importance. The wetlands and their contributing drainage areas (see

140 Section 2.2.1 for specific definition) within the subbasins monitored by the ten hydrological stations

141 range from 14 to 23% and from 39 to 56% respectively, demonstrating the large wetland coverage of

142 the NRB and its sub-basins (Table 1). The lower NRB is an important agricultural area of the Songnen

143 Plain, which is one of the three major plains (including the Sanjiang, Songnen and Liaohe Plains) in

144 northeast China. Therefore, understanding potential floods and hydrological droughts under future

145 climate change is crucial for ensuring regional food security and wetland ecological integrity. During

146 the past 60 years, land use and land cover types have drastically changed owing to large-scale

147 development of intensive agriculture and water resources management (Meng et al., 2019). The area of

148 wetlands in the NRB decreased by nearly 23% from 1978 to 2000 (Chen et al., 2021), with only 16.34%

149 remaining today (Table 1), which largely degraded their services (Wu et al., 2021). Along with the

150 reduction in wetland area, the hydrological functions of wetlands in the NRB, such as water storage,

151 flood mitigation and baseflow support, have been considerably reduced (Wu et al., 2021). These wetland

152 services are closely related to flood and drought risks, such as the 1998 mega-flood. In order to

153 effectively deal with the risk of floods and droughts, the Nierji Reservoir was constructed along the

154 mainstream NRB (Fig. 1); it started normal operation in 2006. The drainage area of the reservoir

155 accounts for 22.8% of the NRB. The Nierji Reservoir, located in the upper Nenjiang River (Fig. 1), has

156 flood control and water supply as the primary purposes and hydropower generation and navigation as

157 secondary purposes, thus playing an important role in the distribution of water resources for the lower

158 NRB.
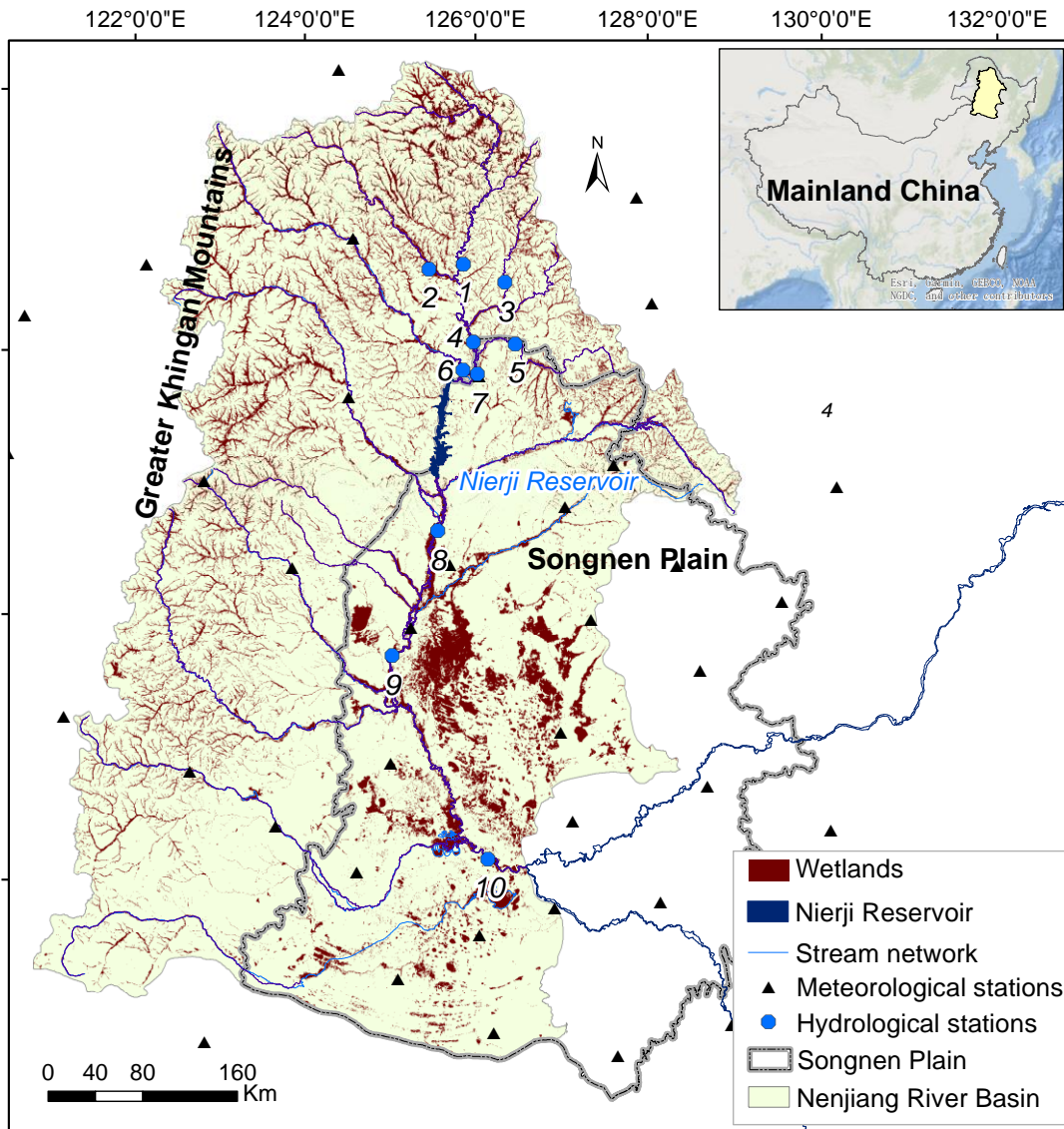
160 Figure 1. Location of the Nenjiang River Basin and the distribution of wetlands, river networks, Nierji

161 Reservoir, and hydrological and meteorological stations within the basin.

162

163 Table 1 The drainage area of the ten hydrological stations used in this study, area ratios of wetlands and

164 their contributing areas to the drainage area of the Nenjiang River Basin, northeast China.

ID	River	Hydrological stations	Drainage area (km^2)	Wetland area ratio (%)	Wetland contribution area ratio (%)
1	Mainstream	Shihuiyao	17205	22.2	54.7

2	Duobukuli River	Guli	5490	16.3	57.1
3	Menlu River	Huolongmen	2151	20.8	50.7
4	Mainstream	Kumotun	32229	20.4	54.3
5	Keluo River	Kehou	7310	23.4	56.2
6	Gan River	Liujiatun	19665	13.2	49.9
7	Mainstream	Nenjiang	61249	18.3	54.1
8	Mainstream	Tongmeng	108029	13.1	47.5
9	Mainstream	Fulaerji	123911	13.7	39.0
10	Mainstream	Dalai	221715	16.3	42.4

The driving datasets used in this study include meteorological data, land-use/land-cover types, soil texture, digital elevation models, drainage network, and observed discharge data. The land-use/land-cover types for 2015 (including wetland types), digital elevation models and digital elevation models with 1 km resolution were obtained from Resource and Environment Science and Data Center (https://www.resdc.cn/). The river network was collected from the Geographical Information Monitoring Cloud Platform (https://www.dsac.cn/DataProduct/Index/30). Historical daily meteorological datasets including precipitation and air temperature for the period 1963-2020 were obtained from 39 weather stations administered by the National Meteorological Information Centre of China (http://data.cma.cn) and 49 weather stations in the upper NRB (Fig. 1) administered by the Nenjiang Nierji Hydraulic and Hydropower Ltd. Company (http://www.cnnej.cn). The hydrological data from ten hydrological stations (see Fig.1 and Table 1) were obtained from the Songliao Water Resources Commission, Ministry of Water Resources (http://www.slwr.gov.cn/), with the time series extending from 1963 to 2020.

In this study, we drove hydrological model using five GCM projections (GFDL-ESM4, IPSL-CM6A-LR, MPI-ESM1-2-HR, MRI-ESM2-0, UKESM1-0-LL) under three Socioeconomic Pathways (SSPs) from the latest CMIP6 (O'Neill et al., 2016). Each of these specific SSPs represents a development model that includes a corresponding combination of development characteristics and influences. The

183   three SSPs that were used herein include SSP126, SSP370 and SSP585, which represent potential

184   futures characterized by green-fueled growth (van Vuuren et al., 2017), high inequality between the

185   countries (O'Neill et al., 2016) and fossil-fueled growth (Kriegler et al., 2017), respectively. We chose

186   the five GCM projections because their high resolution (0.25°) and wide application in previous studies.

187   Given the data requirements of the hydrological model, we downloaded the SSP outputs including daily

188   precipitation, maximum and minimum temperature. We then performed bias correction and spatial

189   downscaling of the SSP outputs. The bias correction of SSP outputs was carried out using the CMhyd

190   software (https://swat.tamu.edu/software/cmhyd), in which the widely used Delta Change method in the

191   CMhyd software was adopted. Delta Change bias-corrects the projected SSP outputs based on the

192   historical statistics and thus conserves the linear spatial-, temporal-, and multi-variable dependence

193   structure in the future climate (Bosshard et al., 2011; Maraun, 2016; Moore et al., 2008; Shafeeque and

194   Luo, 2021). The ANUSPLIN package developed by (Hutchinson and Xu, 2004) was then used to

195   uniformly downscale the output from five bias-corrected GCMs to a resolution of 1-km based on the

196   DEM. Following previous studies (Hagemann and Jacob, 2007; Zhao et al., 2021), the multi-model

197   ensemble means (M_{GCM}) of the daily precipitation, and the maximum and minimum temperature under

198   the SSPs scenarios were then obtained to diminish the uncertainties inherited in a single GCM. MEM

199   was calculated using an equally-weighted average:

200
$$M_{GCM} = \frac{1}{N} \sum_{i=1}^{N} P_i \qquad (1)$$

201   where M_{GCM} is the multi-model ensemble means, N is the number of ensemble members (5 in this study);

202   and P_i is the projected climate data of an ensemble member. In this study, the M_{GCM} of five GCMs were

203   used to drive hydrological modeling.

204   2.2. Framework of hydrological modeling coupled with wetland modules and reservoir operation

205   scenarios

206   We developed a spatially-explicit hydrological modeling framework that considers wetland

207   hydrological processes and reservoir operations based on HYDROTEL model and reservoir simulation

208   algorithms (Fig.2). Such a modeling framework was based on a distributed coupling implementation at

209 watershed scale from upstream to downstream. Observed streamflow from seven hydrological stations

210 (see hydrological stations 1-7 in Fig.1) located upstream of the Nierji Reservoir and three hydrological

211 stations (see hydrological stations 8-10 in Fig.1) installed at downstream of the reservoir, respectively,

212 were used to calibrate the HYDROTEL model. For the upstream Nierji Reservoir, we calibrated the

213 HYDROTEL model against observed streamflow of seven hydrological stations with consideration of

214 wetlands (i.e., hydrologic-wetlands model). Among the seven hydrological stations, the Nenjiang

215 Station is located at the end of the upstream, where the simulated streamflow was taken as the inflow of

216 the reservoir. We then computed the reservoir outflow using the simulated inflow, estimated lateral

217 inflow and reservoir simulation algorithms (see Section 2.2.2), thereby integrating reservoir operation

218 into the hydrologic-wetlands model to build a hydrologic-wetlands-reservoir model. Based on the

219 calibrated hydrologic-wetlands-reservoir model, we simulated the outflow of the reservoir (Sect. 2.2.2),

220 which was used as the input streamflow for downstream model calibration. For the downstream reservoir,

221 we calibrated the hydrologic-wetlands-reservoir model against observed streamflow of Tongmeng,

222 Fulaerji and Dalai Stations. Based on this framework, the simulation of basin hydrological processes

223 coupled with basin scale wetlands and reservoir operations were realized.
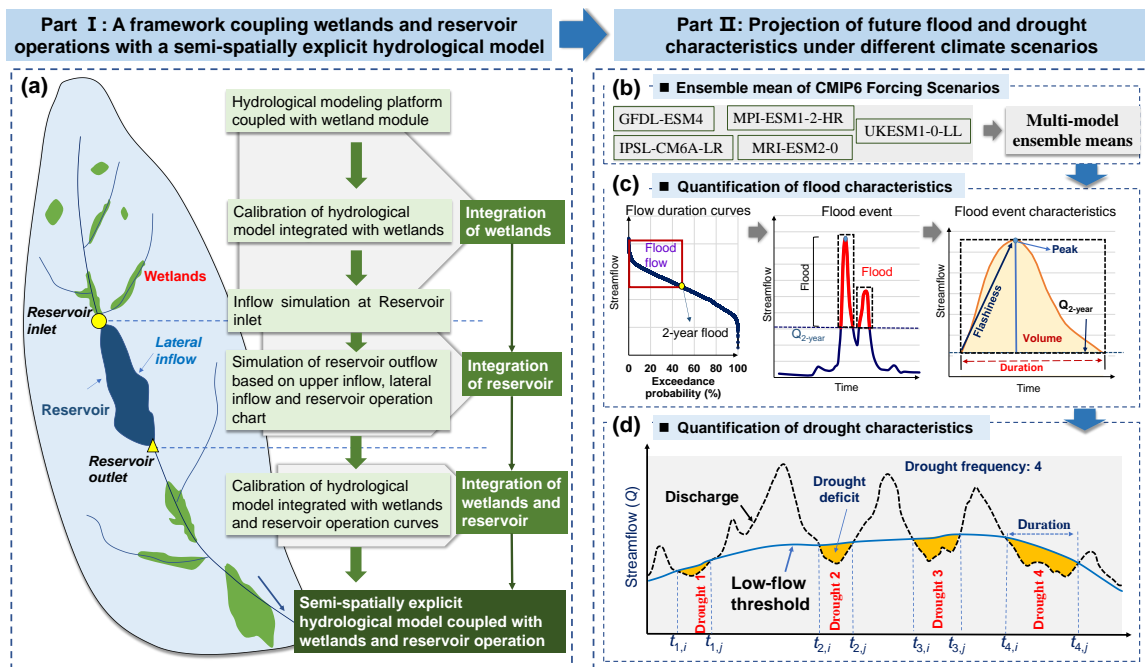
224

225 Figure 2. Framework for projecting future flood and hydrological droughts based on a semi-spatially

226　integrating wetlands and reservoir operation into a basin hydrological model: (a) a framework coupling

227　wetlands and reservoir operations with a semi-spatially explicit hydrological model; (b) multi-model

228　ensemble means from five GCM projections used for driving modeling framework; (c) methodology

229　for determining a flood threshold, defining flood events, and extracting flood characteristics, and (d) a

230　sequence of runs with examples of drought deficit, duration, and frequency.

231　2.2.1. A semi-distributed hydrological model platform coupled with wetland modules

232　　The PHYSITEL/HYDROTEL modeling platform coupled with two wetland modules (isolated and

233　riparian wetlands) (Fossey et al., 2015b), has been used to quantify hydrological function of wetlands

234　(e.g., Fossey and Rousseau, 2016; Blanchette et al., 2019; Wu et al., 2023). PHYSITEL is a Geographic

235　Information System based pre-processing platform for managing hydrological modeling data (Noël et

236　al., 2014; Rousseau et al., 2011). Using general basin data (a digital elevation model, vectorized river

237　network and lacustrine water bodies, and raster-based land use and soil matrix distribution maps),

238　PHYSITEL divides the basin into more detailed hydrological response units, i.e., relatively

239　homogeneous hydrological units (RHHUs) (Fortin et al., 2001). The RHHUs were defined using the

240　algorithm for delineating and extracting hillslopes proposed by (Noël et al., 2014). The hillslopes with

241　same characteristics (e.g., physical geography and hydrological response) were then aggregated within

242　each RHHUs. In addition, the PHYSITEL platform distinguishes wetlands from other land-use types,

243　and then classifies both isolated and riparian wetlands based on an adjacency threshold (i.e., percentage

244　of pixels in contact) between the wetlands and the river network (Fossey et al., 2015b). Specifically, if

245　more than adjacency threshold (e.g., 1%) of wetland pixels are connected to the river network, they are

246　considered as pixels of a riparian wetlands; otherwise, they are referred to as isolated wetlands. It

247　subsequently generates data pertaining to isolated and riparian wetlands and their contributing areas.

248　The contributing area of wetlands is defined as the sum of the area of all wetland RHHUs and upland

249　RHHUs within their immediate catchment areas situated along active fill-spill pathways to the stream

250　network (Evenson et al., 2016). The PHYSITEL platform uses the concept of a hydrologically

251　equivalent wetland (HEW) proposed by (Wang et al., 2008) to integrate isolated and riparian wetlands

252　at the RHHU scale. These typically large RHHUs contain large wetland complexes consisting of various

253 wetland categories such as bogs, fens, marshes, and forested peatlands. After defining the hydrological

254 and wetland parameters, PHYSITEL can directly export the database as part of the input data to

255 HYDROTEL; these data can also be used for other watershed hydrological models.

256 HYDROTEL is a physically-based and semi-distributed hydrological model (Bouda et al., 2014;

257 Bouda et al., 2012; Turcotte et al., 2007) that requires wetland parameter data, land-use type maps, soil

258 texture maps, meteorological data (e.g., daily temperature and precipitation) and daily flows as input.

259 The HYDROTEL model couples the hydrological processes associated with both isolated and riparian

260 wetlands (i.e., the isolated and riparian wetlands modules) at the RHHU scale and calculates the wetland

261 water balance with respect to the surface area of the HEW, contribution area and RHHU. Specifically,

262 for isolated wetlands, the hydrogeological processes are integrated in the vertical water budget (Fortin

263 et al., 2001) at the RHHU scale. For riparian wetlands, the water balance is partially integrated in the

264 vertical water budget of an RHHU and directly connected to the associated river segment via the

265 kinematic wave equation (Beven, 1981). Based on this, the isolated wetlands modules can realize the

266 vertical water balance processes of hillslope wetlands with land surface runoff processes, while the

267 riparian wetlands modules can realize the interaction of hydrological processes between riparian

268 wetlands and river channels. It should be mentioned that the HEW concept developed by Wang et al

269 (2008) served as the foundation for the integration of riparian wetlands and isolated wetlands into the

270 modeling framework. This concept contends that the features of one HEW (also known as an isolated

271 wetland or riparian wetland) are equivalent to the sum of the characteristics of each wetland inside a

272 RHHU (which could either be hill slopes or elementary sub-watersheds related to one river segment).

273 The following premises apply to this concept: (i) only one isolated and/or riparian HEW per RHHU; (ii)

274 one HEW can be fully integrated within a RHHU; (iii) isolated HEW parameters must be numerically

275 integrated; and (iv) riparian HEW parameters must be numerically integrated and spatially integrated

276 (i.e., located in a specific location on the river segment). Therefore, isolated wetlands and riparian

277 wetlands do not appear to have direct hydrological connection within a RHHU. However, isolated

278 wetlands also have hydrological interactions with riparian wetlands through vertical water balance

279 processes and fill-spill processes (Fossey et al., 2015). Nevertheless, such representations provide a

280 modelling approach that can simulate water balances at the wetland scale while considering their

281 interactions with the surrounding environment (contributing drainage area and hydrological

282 connectivity) (Fossey et al., 2015b). But the hydrological interactions between riparian wetlands and

283 isolated wetlands are not considerate in this study.

284 2.2.2. Simulation of Nierji reservoir operations

285 Based on the simulated runoff at the inlet (the Nenjiang Station), lateral inflow, and the schemes of

286 reservoir operation, we estimated the reservoir outflow using the ResSimOpt-Matlab software package

287 developed by Dobson et al., 2019. ResSimOpt-Matlab contains three algorithms for reservoir simulation.

288 The first algorithm considers a case when we want to always release a constant amount over the

289 simulation period. This constant amount is the target release that would cover all downstream demand

290 for water, for instance for domestic use and/or irrigation. The second consider a case when we still want

291 to release the target demand but we would also like to (1) apply some hedging (that is, an intentional

292 reduction of the release - even if it would still be feasible to release the target demand - aimed at saving

293 more water and thus facing smaller deficits at later time); and (2) attenuate downstream peak flows for

294 flood control purpose. The third algorithm, which was used in this study, dynamizes the operation rules.

295 A dynamic operation schemes was used in this study to achieve the simulation. Specifically, following

296 (Dobson et al., 2019) and according to actual hydrological conditions, we defined two seasons: the wet

297 season (from June to September) when the risk of flooding is higher and we wanted to release the target

298 demand and provide some storage space for flood control, and the dry season when the risk of flooding

299 is low and the main objective is to sustain ecological baseflows. The required input data to the algorithm

300 includes reservoir inflow (Q_{in}) (m^3/s), the minimum environmental flow (E_{env}), (m^3/s) initial storage (S_o)

301 (m^3), minimum (S_{min}) and maximum (S_{max}) storage (m^3), estimated evaporative losses (E_{vap}) (mm),

302 released discharge (Q_{out}) (m^3/s) and the simulation time-step length (day). Based on the required data,

303 we performed reservoir simulation by implementing the mass balance equation at each simulation time

304 step t:

305
$$\begin{cases} S_{(t+1)} = S_{(t)} + Q_{in(t)} - E_{vap(t)} - Q_{out(t)} \quad or \quad S_{(t)} + Q_{in(t)} - E_{\min(t)} - E_{vap(t)} \\ 0 \le S_{(t)} \le S_{\max} \\ 0 \le R_{(t)} \le \min\left(S_{(t)} + Q_{in(t)} - E_{\min(t)} - E_{vap(t)}, Q_{\max}\right) \end{cases}$$ (2)

306   where S_t is the reservoir storage at time t. S_t and Q_{out} are constrained by the design specifications

307   and operation rules of a reservoir. Specifically, S_t cannot exceed the reservoir capacity $S_{\max}$, while

308   Q_{out} (m^3/s) is constrained by the operation schemes and capacity of the turbines $Q_{\max}$ (m^3/s). The

309   excess water, if any, is spilled:

310
$$Q_{spill(t)} = \max\left(S_{(t)} + Q_{in(t)} - E_{vap(t)} - Q_{out(t)}\right)$$ (3)

311   Based on this, the dynamic Q_{out} can be represented using the equation (1) and (2).

312   We collected information on the reservoir operation including reservoir capacity, control water levels,

313   outflow, the storage-area-water level relationship, the tailwater level-discharge relationship, and the

314   maximum release, along with other data necessary to estimate the outflow. The reservoir inflow is the

315   simulated streamflow at the Nengjiang Hydrological Station, which is at the inlet of the Nierji Reservoir.

316   The minimum storage and maximum storage are 4.9 billion m^3 and 86.1 billion m^3, respectively. Based

317   on the available data for the study area, the Karrufa method (Kharrufa, 1985) was used to estimate daily

318   evaporative losses from the reservoir. We convert days to seconds so that it would correspond to the

319   flow data. During the wet season, the actual operation schemes for the Nierji Reservoir are as follows:

320   The pre- and post-flood periods are June 1-20 and September 6-30, respectively, with a flood limited

321   water level of 216.0 m; The main flood period is from June 21 to August 25, and the reasonable flood

322   limited water level ranges from 213.4 m to 216.0 m and can be gradually increased. During the dry

323   season, the environmental flow was defined as 25.3% of the daily streamflow during the dry season

324   over the years based on the designed operating curves of the reservoir operation chart.

325   2.2.3. Model calibration, validation and performance assessment

326   For all above scenarios, we calibrated the HYDROTEL model against observed streamflow at a daily

327   time step over 8 years, including a 1-year warm-up (2010.10.01-2011.09.30) and a 7-year calibration

328   (2011.10.01-2018.09.30) periods. The same model settings (i.e., key parameters, simulation periods,

329 fitting algorithm, and objective function, etc.) were used for the calibration processes under the both

330 presence and absence scenarios. Following (Arsenault et al., 2018), the model was calibrated using full-

331 time observations without additional validation, as the former allows for more reliable parameters and

332 maximizes the accuracy of the model. The dynamically dimensioned search algorithm (DDS) developed

333 by (Tolson and Shoemaker, 2007) was used to calibrate the 13 most sensitive parameters of the model

334 as proposed by (Foulon et al., 2018). Based on the maximizing of Kling-Gupta efficiency (KGE) (Gupta

335 et al., 2009), automatic calibrations using DDS were carried out utilizing 10 optimization trials (250 sets

336 of parameters per trial). Then, the best set of parameter values out the 10 trials were selected following

337 (Foulon et al., 2018). The KGE was chosen as the objective function because previous research has

338 shown that it can improve flow variability estimates when compared to the Nash-Sutcliffe efficiency

339 (NSE) (Fowler et al., 2018; Garcia et al., 2017).

340 It should be noted that we calibrated the HYDROTEL model against observed streamflow under with

341 and without wetland scenarios. For the without wetland scenarios are defined as follows: When the

342 wetland modules are turned off in HYDROTEL, wetland areas are not removed, but they are treated as

343 the land cover of saturated soils. Such a saturated soil is fixed and does not participate in hydrological

344 processes such as water yielding and runoff routing, and thus their explicit storage properties are not

345 accounted for in the modeling. This is a basic assumption that has been used in several studies using

346 models such as SWAT (Liu et al., 2008; Wang et al., 2008; Evenson et al., 2015), Mike 11 (Ahmed,

347 2014) and HYDROTEL (Fossey et al., 2016; Fossey and Rousseau, 2016a, b; Wu et al., 2019, 2020a,

348 2021), to quantify the hydrologic services provided by wetlands (flood mitigation, flow regulation and

349 baseflow support etc.).

350 To determine whether coupling the wetland module and the reservoir can improve the model

351 performance, we compared (1) the efficiency of the model in simulating daily flow processes; and (2)

352 the capability of the model to simulate floods and hydrological droughts in the presence or absence of

353 the wetlands and the combination of wetlands and reservoir. Following the recommendations of (N.

354 Moriasi et al., 2007) and (Moriasi et al., 2015), four performance criteria were selected to assess model

355 performance with regards to simulated daily flows with and without the presence of the wetland modules

356   and reservoir operation, namely the NSE (Nash and Sutcliffe, 1970), Correlation Coefficient (CC), the

357   root-mean square error (RMSE) and the percent bias (Pbias). We used multiple performance criteria

358   because it may be unreliable to rely on a single objective function to determine whether the model

359   performs well (Fowler et al., 2018; Pool et al., 2018; Seibert et al., 2018). It should be noted that although

360   NSE as an objective function has shortcomings in model calibration, it can still provide an important

361   reference for the evaluation of simulation results as a performance criterion as suggested by Moriasi et

362   al. (2007, 2015). In addition, we compared model performance considering daily hydrograph changes.

363   Furthermore, flood and drought features were extracted (see Sect. 2.4.2 and 2.4.3) and used to discern

364   whether, and to what extent, the coupled wetland modules and reservoir simulations could improve the

365   model's ability to simulate droughts and floods.

366

367   2.3. Projection of future flood and drought characteristics under different climate scenarios

368   The calibrated hydrologic-wetland-reservoir model was used to simulate streamflow driven by multi-

369   model ensemble means from the latest CMIP6 and to derive drought and flood characteristics. The flood

370   and drought characteristics were then compared against historical periods (1971-2020) to discern how

371   future hydrological extremes will be changed under the influence of wetlands and reservoirs (see Part

372   II in Fig.2).

373   The future simulated streamflow at the Nenjiang and Dalai hydrological stations driven by the

374   ensemble mean of bias-corrected CMIP6 Forcing Scenarios (see Section 2.1) were selected to derive

375   drought and flood characteristics. The Nenjiang Station was chosen because it is located at the outlet to

376   (mouth of) the upper NRB and the inlet to the Nierji Reservoir, whose flood and drought patterns are

377   mainly driven by wetlands and climate change. Moreover, changes in drought and flood characteristics

378   of the Nenjiang Station are critical to the operation of the reservoir immediately lower reach. The Dalai

379   Station, located at the outlet of the entire NRB, was used as a proxy to characterize future flood and

380   drought evolution for the whole basin under the combined influence of the wetlands and reservoir. Using

381   the calibrated hydrologic-wetland-reservoir model, we carried out the simulation of hydrological

382   processes for the historical period and under the constraints of the SSP126, SSP370 and SSP585

383   scenarios. We then extracted flood and hydrological drought characteristic indices from the simulations

384   to conduct a comparative analysis of their temporal evolution for the near-future (2026-2050), mid-

385   century (2051-2075) and end-century (2076-2100). The purpose of subdividing the analysis into three

386   time periods was to compare whether, or to what extent, flood and drought characteristics increase or

387   decrease for different future time periods as compared to a historical period.

388   In this study, we characterized floods in terms of four indices consisting of flood peak, flood volume,

389   duration, and flashiness (Fig. 2c). The 2-year flood streamflow was used as a threshold for defining

390   flood events, as it has been often used as a substitute of the threshold for bankfull discharge in previous

391   studies (Cheng et al., 2013; Wu et al., 2020; Xu et al., 2019). Daily streamflows that were greater than

392   the 2-year flood threshold were considered as flood flows. Flood flows occurring on multiple

393   consecutive days were considered as a single flood event. The flood indices, i.e., flood peak, volume,

394   duration, and flashiness were derived with respect to event hydrographs. Flood volume is the cumulative

395   flow from the initial to the end of a flood event with respect to the 2-year flood streamflow level, and

396   represents the flood intensity for different flood events (Wang et al., 2015). The annual total flood

397   volume is the total amount of water associated with all flood events during a water year. We calculated

398   the annual total flood volume based on flood duration and the average amount of streamflow per event

399   in a water year. Flood duration varies for different floods and is, therefore, an important characteristic

400   of a flood event. We summed the flood duration of each event in a water year to obtain the annual flood

401   days. In addition, the annual maximum peak flow was derived from the daily flows to investigate

402   changes in the characteristics of extreme floods. We extracted the 2-year flood threshold for a

403   hydrological station based on the streamflow-exceedance probability curve. Flashiness is a measure of

404   flood severity and is defined as the difference between the peak discharge and action stage discharge

405   normalized by the flooding rise time (Saharia et al., 2017).

406   We characterized hydrological drought characteristics using four indices consisting of the number of

407   droughts, annual drought days, drought duration and deficit (Fig. 2d). A threshold method was used to

408   define hydrological drought events because it can determine the start and end of a hydrological drought

409   event, which allows further assessment of drought characteristics, such as frequency, duration, and

410 intensity of a drought event (Cammalleri et al., 2017). It is based on defining a flow threshold (discharge,

411 Q, m^3/s), below which a hydrological drought event is considered to occur (also known as a low flow

412 spell). A daily variable threshold, defined as an exceedance probability of the 365 daily flow duration

413 curves was used to derive drought events from daily streamflow records (Fleig et al., 2006; Hisdal and

414 Tallaksen, 2003). For rivers with perennial flow, relatively low streamflows ranging from Q_{70} to Q_{95}

415 have been used as a reasonable threshold (Tallaksen and van Lanen, 2004; Zelenhasić and Salvai, 1987).

416 In this study, we chose the 90th percentile (Q_{90}-n) streamflow as the daily threshold, which also used as

417 the threshold for identifying droughts in future climate change scenarios. The Q_{90}-n of all days was

418 determined based on the observed historical daily streamflow.

419   To enable the comparison across different modeling scenarios (i.e., historical scenarios and future

420 climate change scenarios), we derived drought days, deficit, duration, and number from identified

421 hydrological drought events to characterize their patterns. Drought volume deficit was calculated by

422 subtracting daily streamflow from the threshold level (Q_{90}-n) during a drought event, and it presents the

423 severity of the drought compared to the normal streamflow conditions. Drought duration was the

424 cumulative number of days during a drought event, i.e., the number of days from the beginning to the

425 end of the drought. Annual drought days were then the cumulative drought duration in a year. The

426 number of droughts is expressed by the number of drought events during a study period. In addition, the

427 annual minimum flows of each water year were extracted and used to determine the model's ability to

428 simulate very low flows. The drought volume deficit was calculated as:

429
$$D_k = \sum_{t_i}^{t_j} \left(Q_{90,t} - Q_n \right) \cdot 60 \cdot 60 \cdot 24 \tag{4}$$

430 where D_k is the drought volume deficit (m^3) of a drought event k at a hydrological station and $t_{k,i}$ and $t_{k,j}$

431 are the initial and final time steps of the run, respectively. Q_n is the daily streamflow of n day of the year

432 (1-365). The corresponding drought duration is computed as t_j-t_i +1.

433   For hydrological drought events that occur relatively close in time, the inter-event time method

434 introduced by (Zelenhasić and Salvai, 1987) was used to separate events. This method defines a

435 minimum gap period, t_c, and assumes that if the inter-event time (t_j-t_i+1) < t_c, then the consecutive events

436   are interdependent and merged. In this case, the total drought deficit volume is the sum of the individual

437   deficit values, and the event duration is the so-called real drought duration (sum of the single event

438   duration, excluding excess periods). For this study, t_c was set equal to 7 days as recommended by

439   (Cammalleri et al., 2017).

440

441   **3. Results**

442   3.1 Model performance on daily streamflow and hydrography

443   Fig. 3 depicts model performances for calibration results in the presence or absence of the wetlands

444   and the combination of wetlands and reservoir at the ten hydrological stations in the NRB. In the case

445   of whether the wetlands were present or absent, the simulated daily streamflow results all achieved the

446   acceptable performance criteria (NSE > 0.5 and Pbias ≤±15%) suggested by (Moriasi, 2007) and

447   (Moriasi et al., 2015) at the Shihuiyao, Guli, Huolengmen, Kumotun, Kehou, Liujiatun and Kumotun

448   stations. However, compared with the calibrated results of the model without wetlands, the simulation

449   efficiency under with wetland scenario improved to varying degrees. Specifically, the relative

450   improvement (i.e., the relative change) of KGE values at Shihuiyao, Guli, Huolengmen, Kumotun,

451   Kehou, Liujiatun, Kumotun, Tongmeng, Fulaerji and Dalai were 44%, 24%, 2%, 6%, 5%, 3%, 4%, 46%,

452   47% and 67%, respectively. In addition, the NSE and CC values were generally larger in the presence

453   of wetlands than those in the absence of wetlands, and the RMSE and Pbias values are generally smaller

454   than those in the absence of wetlands, showing that integrating wetlands into the hydrological model

455   can slightly improve the model calibration results.
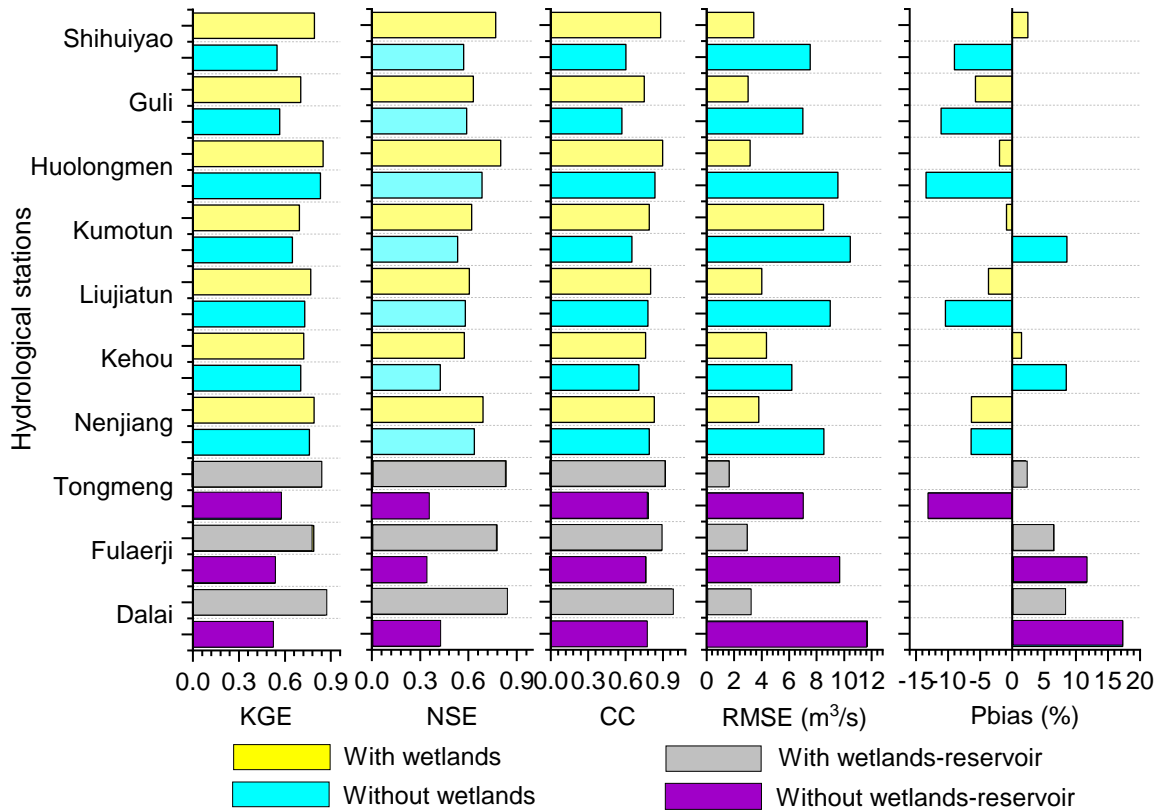
Figure 3. Model performances for calibration results for the with/without wetlands and reservoir

scenarios at the ten hydrological stations in the Nenjiang River Basin. The KGE, NSE, CC, KGE,

RMSE and Pbias refer to Kling-Gupta efficiency, Nash-Sutcliffe efficiency, Correlation Coefficient,

Root Mean Square Error, and the percentage bias, respectively.

    For the lower reaches of Nierji Reservoir (i.e., the Tongmeng, Fulaerji and Dalai stations, representing

inclusion of the wetlands and the reservoir operation into hydrological modeling), the NSE and CC

values were greatly higher and RMSE and Pbias values were substantially lower when the wetlands and

reservoir were considered, in comparison to the case without wetlands-reservoir (Fig. 3). In fact, in the

scenario without wetlands-reservoir, the simulated daily streamflow results failed the acceptable

performance criteria (NSE > 0.5 and Pbias ≤±15% as suggested by Moriasi (2007) and Moriasi et al.

(2015). In addition, the simulated daily streamflow in the no-wetland and no wetlands-reservoir

scenarios both overestimated the high flows, especially those during the flood periods; during the low

flow periods, the low flows were underestimated (Please refer to Fig. A1 in Supplementary materials).

471   Further, the simulated hydrographs under the wetland and wetlands-reservoir scenario were in much

472   better agreement with the hydrographs of observed streamflow, especially during floods and the low-

473   flow period (Please refer to Fig. A2 in Supplementary materials). These results indicate that inclusion

474   of the wetlands and the operation of reservoirs can greatly improve model capacity to replicate basic

475   hydrograph characteristics and capture hydrological extremes (e.g., high and low flows).

476   3.2 Model capacity to replicate flood and drought characteristics

477   The simulated annual minimum streamflow for the wetlands/wetlands-reservoir scenarios were, in

478   general, slightly overestimated or approximately equivalent to the observations compared to the

479   scenarios that did not include the wetlands/wetlands-reservoir (Fig. 3). However, the simulation results

480   without wetlands clearly underestimated minimum streamflow, distinctly overestimated annual drought

481   days and drought deficit compared to the simulation results for the scenario with wetlands at the ten

482   hydrological stations. In addition, the simulated annual maximum peak flow, flood days and volume

483   under the with/without wetland scenarios are, in general, approximately comparable to observations at

484   the Guli, Kumotun, Kehou, Liujiatun and Nenjiang hydrological stations (Fig. A4). Specifically, for the

485   upstream Nierji Reservoir, it is apparent that if wetlands are not considered, the number of annual flood

486   days will be overestimated, whereas flood volume will be substantially underestimate at the

487   Huoloengmen Station. For the lower reach of Nierji Reservoir, lack of integrating the wetlands and

488   reservoir into the simulation can lead to a notable underestimation of annual flood days, and a substantial

489   overestimation of the annual maximum peak flow and flood volume. These results demonstrate that

490   integrating wetlands and the combination of wetlands and the reservoir into the model can help improve

491   model performance with regards to flow during the calibration process, and enhances the model's

492   capability of depicting streamflow processes as well as capturing flood and drought characteristics.

493
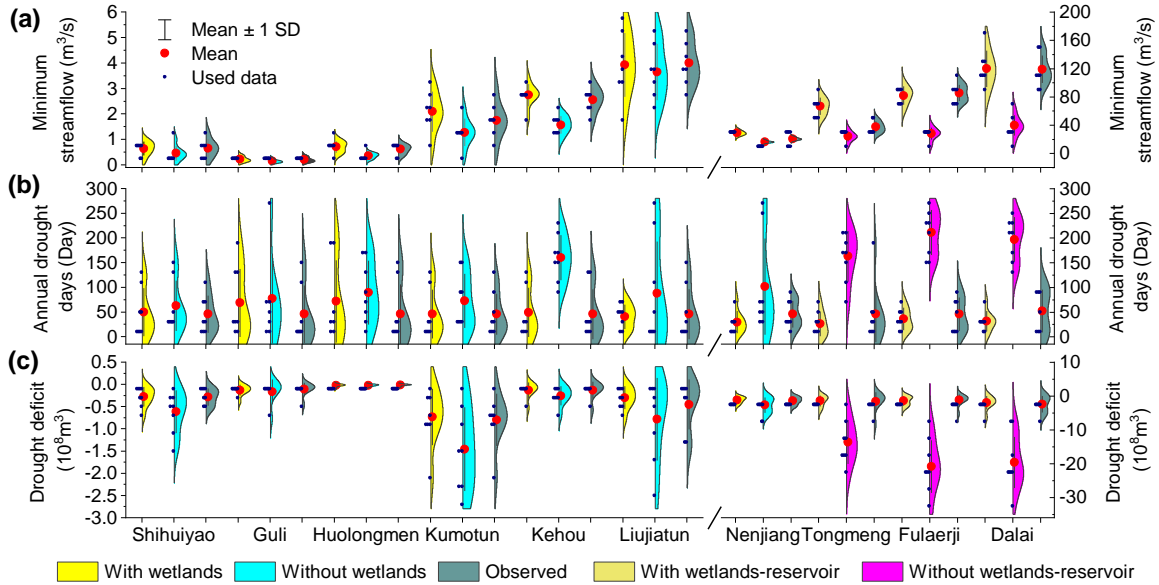
Figure. 3. Annual minimum streamflow, drought days and deficit derived from observed records and simulated streamflow at ten hydrological stations in the Nenjiang River Basin. The with and without wetlands/wetlands-reservoir refers to streamflow simulation based on the presence or absence of wetlands/wetlands-reservoir.
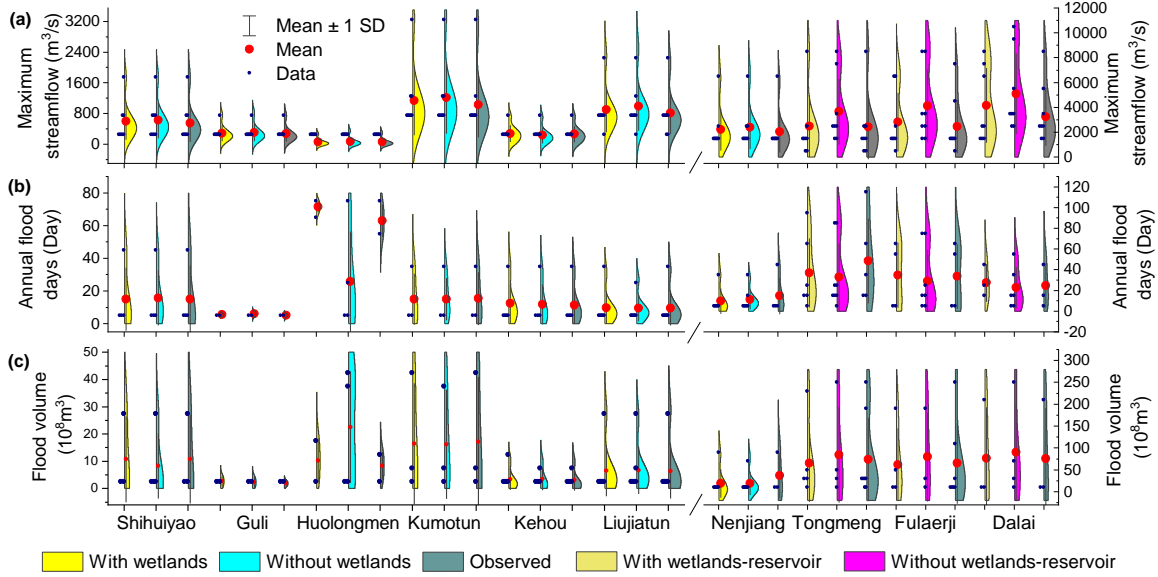
Figure. 4. Annual maximum peak flow, flood days and volume derived from observed records and simulated streamflow at ten hydrological stations in the Nenjiang River Basin. The with and without wetlands/wetlands-reservoir refers to streamflow simulation based on the presence or absence of wetlands/wetlands-reservoir.

3.3 Projection of future floods

A comparison between historical and projected flood characteristics at the Nenjiang Station (representing inclusion of wetlands into hydrological modeling) shows an overall increase in flood risks in the upper NRB. The flood duration, peak flow, volume and flashiness generally exhibit larger fluctuations in most of the scenarios (different SSPs and three periods as shown in Fig. A3 and Table A1). In addition, the averaged increase in flood duration, peak flow, volume and flashiness ranges from 0.9 to 1.2%, from 16 to 33%, from 8 to 111% and from 26 to 55%, respectively (Fig.6). Specifically, the extreme values of flood duration are much larger during the near future and end-century under the SSP126 scenario, the end-century under the SSP370 scenario and the mid- and end-century under the SSP585 scenario (Fig. 6a). Apart from a slight decrease during the near future and mid-century under the SSP585 scenario, peak flow will increase through time in the SSP126, SSP370 and SSP585 scenarios (Fig. 6b). Simultaneously, the flood volume will experience the greatest increase of 68% during the near future under the SSP585 scenario, followed by a 22% increase during the mid-century under the SSP126 scenario (Fig. 6c). In terms of flashiness, the floods will be more severe under the constrains inherent

518   in the SSP126 and SSP585 scenarios and less severe given the conditions in the SSP370 scenario, as

519   compared to the historical period (Fig. 6d).

520   It should be noted that the flood duration, peak flow, volume and flashiness can decrease in the future,

521   as compared to the historical period (Fig.6). For example, flood duration will slightly decrease during

522   the near future and end-century under the SSP126 scenario, largely decrease during the near future under

523   the SSP585 scenario, respectively. Under the SSP585 scenario, the flood peak flow will experience a

524   decrease with the percentage change values of 15% during the mid-century and the volume will reduce

525   26% during near future. In addition, future flood flashiness will be reduced by 49% and 28% in the near

526   future and the end-century under the SSP370 scenario respectively, and by 21% at mid-century under

527   the SSP585 scenario.

528   The changes in the historical and future flood duration, peak flow, volume and flashiness at the Dalai

529   Station (representing inclusion of downstream wetlands and reservoir operation into hydrological

530   modeling) is shown in Fig.A3 and Fig.4 e-h. Similar to the Nenjiang station, the flood duration, peak

531   flow, volume and flashiness at the Dalai station also exhibit divergent change trends across different

532   SSPs and three periods, as compared to the historical periods. Flood duration is projected to increase

533   largely in the near-future period for the SSP126 scenario, both in the mid-century and end-century for

534   the SSP370 scenario (Fig.6e). The peak flow will broadly decrease for the SSP126 scenario, and increase

535   for the SSP370 and 585 scenarios (Fig.6f). Flood volume shows divergent change trends under the three

536   SSPs (Fig.4g). For the SSP126 scenario, flood volume will grow in the near-future and diminish in the

537   mid- and end-century. Flood volume will decrease in the near-future, increase in the mid-century, and

538   increase slightly in the end-century under the SSP370 scenario. However, following an apparent

539   reduction in the near-future, flood volume is anticipated to have no discernible change trend in the mid-

540   century and a clear increasing trend in the end-century for the SSP585 scenarios. Flashiness will be

541   reduced in the near future and will increase in the mid-century and end-century for the SSP126 scenario

542   (Fig.6h). For the SSP370 scenario, flashiness will increase substantially with percentage changes of 204%

543   in the near-future, Moreover, for the SSP585 scenario, flashiness will experience a considerable increase

544   with percentage changes of 109% in the end-century respectively. In terms of the averaged percentage

change values, the peak flow and flood flashiness will overall increase; the flood volume will reduce in the near future and rise in the mid-century and end-century; and flood duration will experience a slight increase to a minor decrease.
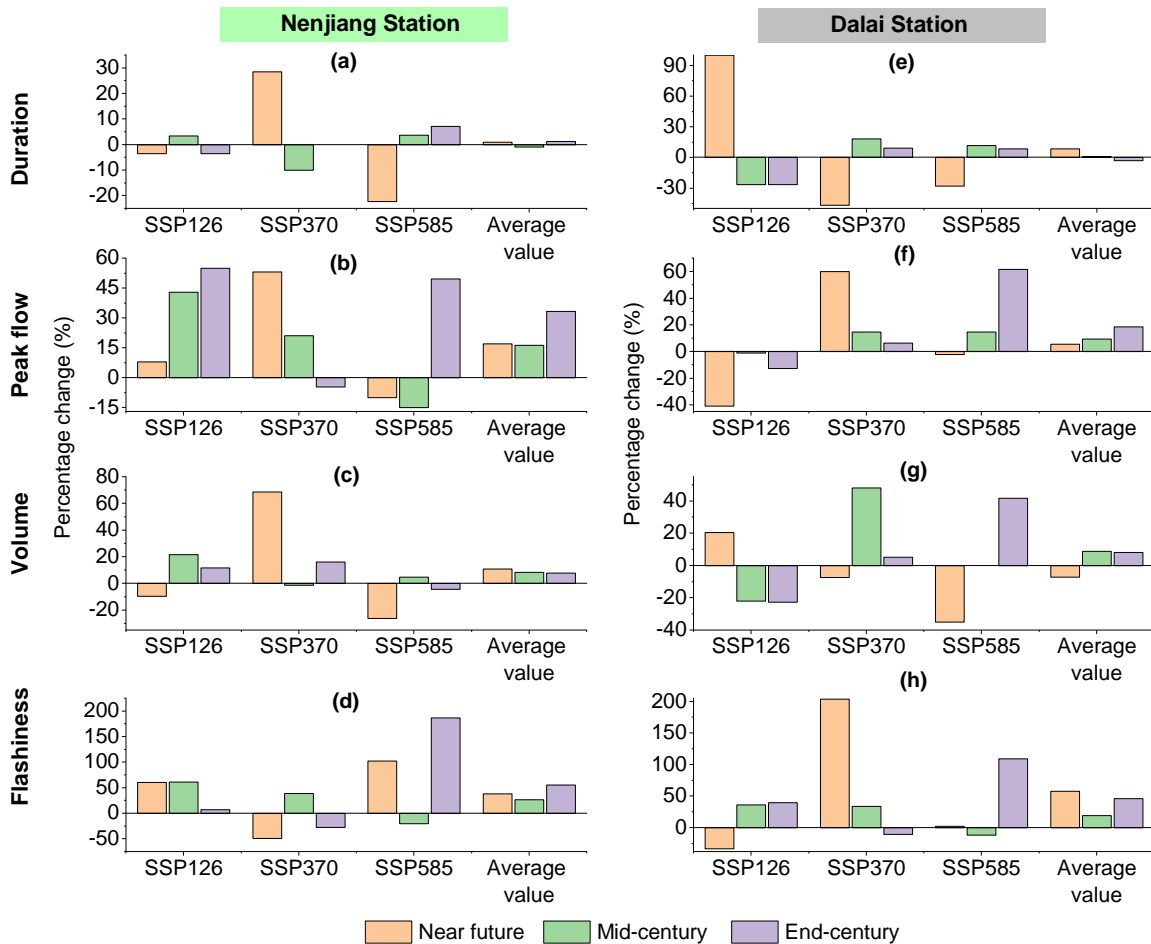

Figure 6. Projected percentage changes (relative to historical period during 1971-2020) in flood duration, peak flow, volume and flashiness at the Nenjiang (the left column) and Dalai (the right column) Station. The near-future, mid-century and end-century refer to the 2026-2050, 2051-2075 and 2076-2100 under the Socioeconomic Pathways (SSP) 126, SSP370 and SSP585 scenarios. The average values were calculated based on the projected percentage changes in the three SSP scenarios.

To further investigate flood risks in the NRB under future climate change, the flood duration-peak flow-flow volume relationships at the Nenjiang and Dalai stations for the SSPs were compared to those

of the historical period and analyzed (Fig. 7a-c). Compared with historical flood risk, extreme flood events with longer and larger volumes will occur more frequently at the Nenjiang Station for the SSP126 and SSP585 scenarios (Fig. 7a and 7c). It is noteworthy that the flood peak-volume-duration relationships between the historical period and SSP370 scenario are approximate equal, with the exception that longer duration and larger volume floods will occur during the end-century period (Fig. 5b). In addition, extreme flood events will occur mainly in the near-future for the SSP126 scenario and during the mid- and end-century for the SSP585 scenario. Moreover, for the SSP370 and SSP585 scenarios, floods will become shorter in duration, and possess a lower peak flow and flood volume in the near-future. Thus, the upper NRB will experience more severe flood events to a large extent under most future climate change scenarios.
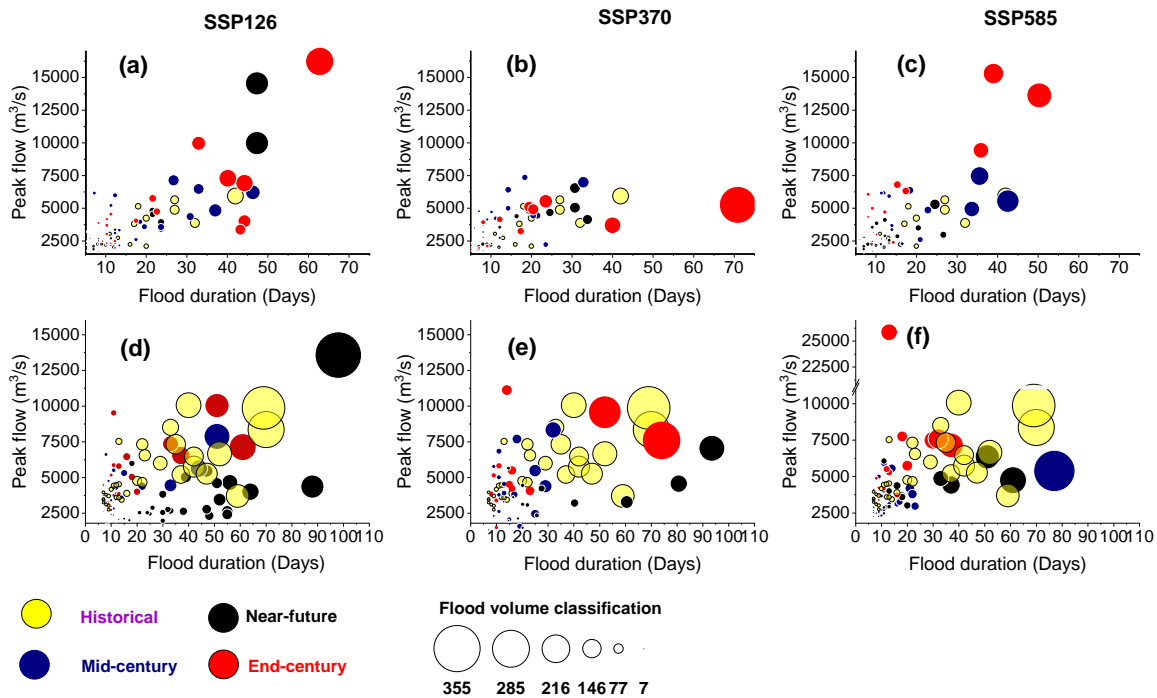
Figure 7. Historical and projected flood duration-peak flow-volume relationships at the Nenjiang (the first row) and Dalai (the second row) Station. The historical period refers to 1971-2020 and the near-future, mid-century and end-century refer to the 2026-2050, 2051-2075 and 2076-2100 under the Socioeconomic Pathways (SSP) 126 (the first column), SSP370 (the second column) and SSP585 (the

26

574   third column) scenarios.

575

576   The duration-peak flow-volume relationships of extreme flood events under future climate change

577   scenarios are closer to those of the historical period at the Dalai Station than at the Nenjiang Station

578   (Fig. 7d-f). For the three future SSPs, the flood events with longer duration, higher peak flows or larger

579   volume than the historical period will occurred infrequently, and the duration, flood volume and peak

580   flow of the other shorter and lower magnitude flood events will generally be attenuated. However, very

581   extreme flood events are projected to occur in the near-future under the conditions of scenario SSP126

582   (Fig. 7d). Likewise, future climate change under the SSP370 scenario and 585 scenarios are projected

583   to result in longer flood events in the near-future and mid-century, respectively (Fig. 7e and 7f).

584   Therefore, the future flood risk can be effectively attenuated to a great extent by the combined influence

585   of wetlands and reservoir. However, extreme floods will still occur in the future.

586   3.4. Prediction of future hydrological droughts

587   The comparison between historical and projected hydrological drought indices shows that the risks

588   of hydrological droughts will be increased to some extent under future climate change for both Nenjiang

589   and Dalai stations. Specifically, in addition to a reduction in the number of droughts and annual drought

590   days in the near future for the SSP126 scenario, the number of droughts (Fig. 8a and 8e), annual drought

591   days (Fig. 8b and 8f) and drought deficit (Fig. 8d and 8h) will overall increase in other periods for three

592   scenarios (Figure A4 and Table A2). It is clear that the number of droughts will be equivalent to the

593   historical period in the mid-century and end-century for the SSP126 scenario and in the mid-century for

594   the SSP585 scenario. For all other scenarios, the number of droughts will increase. In terms of the mean

595   percentage change values, there is a general trend towards an increase in the number of droughts and

596   annual drought days, which indicate that future drought events will be more frequent and there will be

597   more days per year affected by drought. The predicted extreme values show that the future duration of

598   drought at Nengjiang station may shorter than the historical period, but the degree of shortening

599   presented in different SSP scenarios varies (Fig. 8c and 8g). For the Dalai station, the longest drought

600   durations would all exceed historical extremes in the end-century for the SSP126 and SSP585 scenario,

601 and in the near future for the SSP370 scenario. The percentage change values display that drought

602 duration will be reduced at the Nenjiang station and will be extended at the Dalai station for all the SSP

603 scenarios. Drought deficit at the Dalai station will increase by 39%, 36% and 36% and in the near future,

604 mid-century and end-century. For the Dalai station, drought deficit will increase further in the three

605 periods with 39%, 36% and 36%, respectively.

606   A comparison of the percentage change values between the Nengjiang and Dalai stations shows that,

607 apart from a reduction of the number of drought events, the risk of drought to be experienced at Dalai

608 is considerably stronger than at Nengjiang. Specifically, the percentage change in the annual drought

609 days, drought duration and deficit will increase from 85-97% to 89-134%, from -17- -17% to 21%, and

610 from 36-39% to 171-247%, respectively.

611
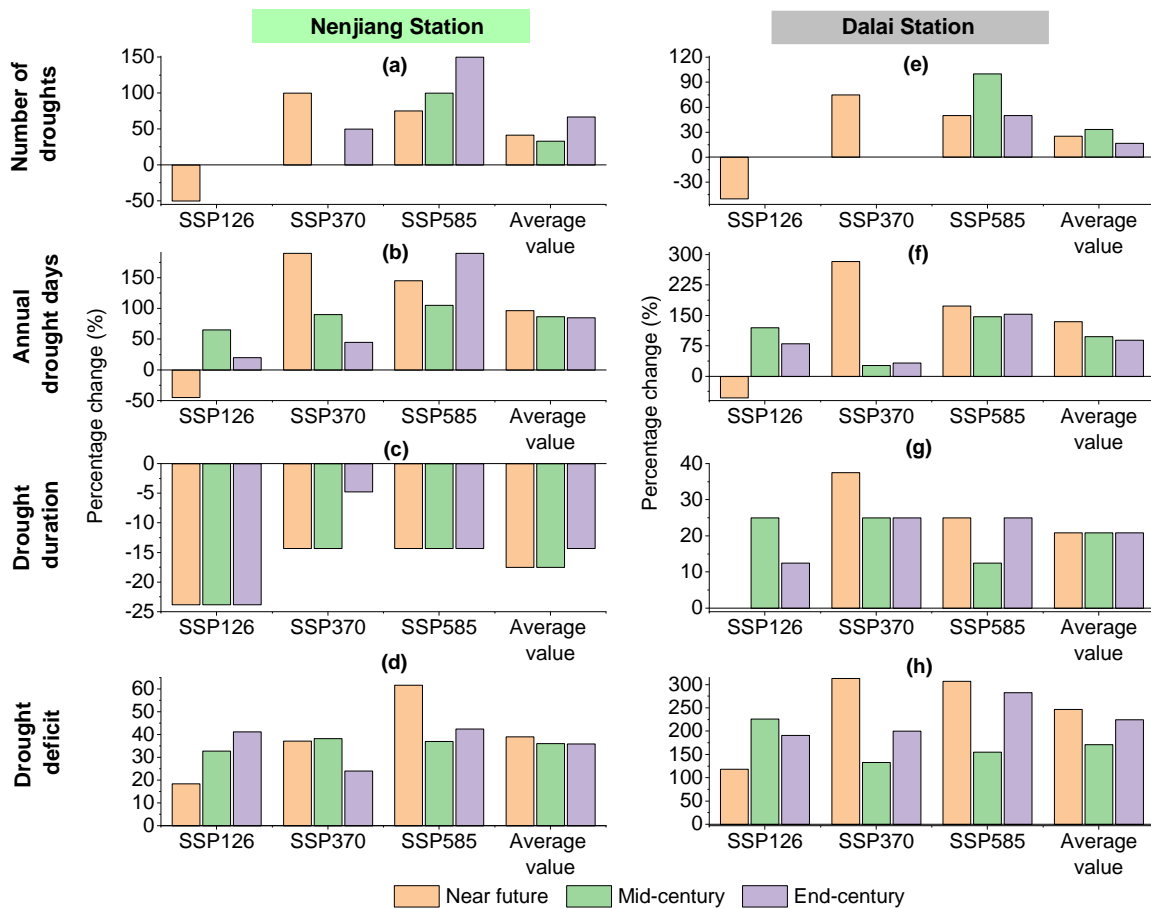
612

613 Figure 8. Projected percentage changes (relative to historical period during 1971-2020) in hydrological

drought characteristics at the Nenjiang (the left column) and Dalai (the right column) Station. The near-future, mid-century and end-century refer to the 2026-2050, 2051-2075 and 2076-2100 under the Socioeconomic Pathways (SSP) 126, SSP370 and SSP585 scenarios. The average values were calculated based on the projected percentage changes in the three SSP scenarios.

To further analyze the temporal evolution of droughts in the Nengjiang River Basin under future climate change, drought events were classified into four types in terms of duration and deficit, i.e., short-term light droughts, long-term light droughts, short-term severe droughts, and long-term severe droughts (see Fig. 9 for details). This four-part classification was then used to compare and analyze the changes in the temporal characteristics of drought events under the different SSP scenarios. Similar to the drought characteristics during the historic historical period, the majority of drought events for the SSP126, SSP370 and SSP585 scenarios are short-term light droughts (Fig. 9a-c), i.e., the upper NRB will still be dominated by short-term light droughts under future climate change. However, these droughts will be slightly aggravated and marginally longer. In addition, long-term light droughts will occur rarely under the conditions inherent in scenarios SSP126 (Fig. 9a) and SSP370 (Fig. 9b), and occur relative frequently in the SSP585 scenario (Fig. 9c). However, compared with the historical period, the overall number of long-term light droughts will largely decrease, but the deficit will increase slightly under future climate change. In addition, short-term severe droughts will increase substantially, along with their deficit. The number of long-term severe droughts for the SSP126 scenario is approximately the same as in the past, but the duration will be substantially reduced. For scenarios SSP370 and SSP585, the number of long-term severe droughts will increase more than during the historical period, but the duration will be markedly less, and the deficit will be reduced to some extent. In terms of the different the sub-periods, severe droughts in the upper NRB will be more severe during the near-future and end-century periods, and relatively less severe in the mid-century period in comparison to the historical period. However, overall, the droughts will be of shorter duration and characterized by an increased deficit under future climates.
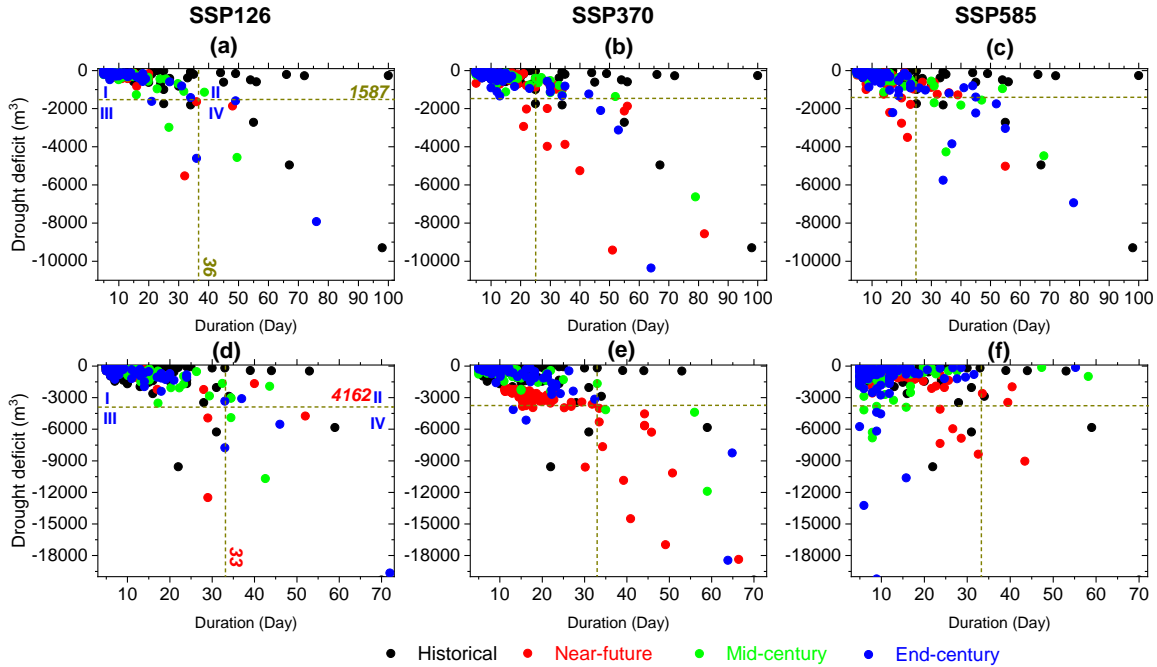
Figure 9. Historical and projected duration-deficit relationship of each hydrological droughts at the Nenjiang (the first row) and Dalai (the second row) Station. The historical period refers to 1971-2020 and the near-future, mid-century and end-century refer to the 2026-2050, 2051-2075 and 2076-2100 under the Socioeconomic Pathways (SSP) 126 (the first column), SSP370 (the second column) and SSP585 (the third column). The dark yellow lines in the horizontal and vertical directions refer the 95% threshold lines for drought deficit and duration values, respectively. I, II, III and IV refer to short-term light droughts, long-term light droughts, short-term severe droughts, and long-term severe droughts, respectively.

Droughts brought about by future climate change at the Dalai Station located along the lower reaches of the NRB will continue to be dominated by short-term slight droughts (Fig. 9d-f). For the SSP126 scenario, the duration and deficit of the short-term slight droughts will be approximately the same as those during historical times (Fig. 9d). However, the duration and deficit of short-term slight droughts will increase given the conditions specified in the SSP370 (Fig. 9e) and SSP585 (Fig. 9f) scenarios. The duration of short-term slight droughts will increase the most for scenario SSP370. In addition, under all three SSP scenarios, long-term slight droughts will, in general, be reduced. In fact, under the SSP370 scenario, long-term slight droughts will not occur. The number of short-term severe droughts will

658　generally tend to increase, with the most pronounced increase under the SSP585 scenario, followed by

659　the SSP370 scenario. A slight increase will occur under the SSP126 scenario. However, long-term

660　severe droughts will increase substantially under the SSP126 and SSP370 scenarios. In particular, under

661　the SSP370 scenario, the duration of long-term severe droughts will be exceptionally prolonged, and

662　the severity will be extraordinarily increased, indicating that the risk of droughts of long duration and

663　with a severe deficit will climb abnormally in some year. For example, under the conditions set by the

664　SSP370 scenario, the deficit of long-term severe droughts will reach -18,169 m^3 and -18,457 m^3 during

665　the near-future and end-century periods. For the SSP585 scenario, long-term severe drought will occur

666　only once in the near-future, which is equivalent to the historical period. These results indicate that the

667　risk of future hydrologic droughts along the lower NRB will further increase even under the combined

668　influence of reservoirs and wetlands.

669

670　**4. Discussion**

671　4.1. Integrating wetlands and reservoir operation into basin hydrologic modeling and basin water

672　management

673　　A series of studies have shown that the simulation and prediction of floods and droughts faces many

674　challenges, such as the scarcity of hydrometeorological driven data (Foulon et al., 2018), model errors

675　(Golden et al., 2021; Smakhtin, 2001; Staudinger et al., 2011) and anthropogenic disturbances (e.g.,

676　reservoir operation) (Brunner, 2021; Brunner et al., 2021). In this study, we developed a spatially

677　explicit hydrological model that considers wetland hydrological processes and reservoir operations

678　through coupling a distributed hydrological modeling platform with wetland modules and reservoir

679　simulation algorithms. We found that coupling wetland alone or coupling wetlands and reservoir with

680　hydrological model can improve model calibration results and model performance of capturing flood

681　and drought characteristics in a large river basin. Such model performance improvement can provide

682　important information for developing downstream water resources management. Previous studies have

683　shown that climate change is further exacerbating the risk of hydrological extremes, leading to an

684   expanding of flood and drought affected area (Diffenbaugh et al., 2015; e.g., Hirabayashi et al., 2013;

685   Wang et al., 2021), which increase the complexity of accurate prediction and the challenge for effective

686   mitigation. Give that, projecting flood and drought risks in response to a changing climate requires

687   robust hydrologic models that take into account the important factors within a watershed that can largely

688   influence basin hydrological processes (Golden et al., 2021).Therefore, in basins that coexist with high-

689   coverage wetlands and multiple reservoirs, it is necessary to integrate wetlands and reservoir operation

690   into basin hydrological simulation, thus providing practical support for extreme hydrological risk

691   mitigation and water resource management under a changing climate.

692   Although our developed framework demonstrates good modeling results, uncertainties could exist in

693   the assessment. Aspects such as the accuracy and error of the input data (Lobligeois et al., 2014), the

694   choice of the objective function (Fowler et al., 2018), the length of the period considered during

695   calibration (Arsenault et al., 2018), and the model structure (Melsen et al., 2019) can all affect the

696   performance of a model to replicate streamflow, thus impacting flood and drought predictions and water

697   management under future climate change. In addition, due to a lack of wetlands water balance

698   monitoring data, this study only used river station data (which only considered the cumulative

699   hydrologic effect of upstream wetlands) for model calibration. Therefore, there are ongoing efforts to

700   obtain sufficient observations on wetland area dynamics and evapotranspiration, water depth and

701   volume, soil water content and actual observations to better calibrate/validate watershed hydrological

702   models, which are expected to better provide key parameters for further improving the model's capacity

703   to capture flood and drought patterns and better serve basin water management. In addition, the several

704   SPPs employed to drive the simulation framework, including SSP126, SSP370, and SSP585 scenarios,

705   can introduce uncertainty into future flood and drought risk projections. Because of the internal

706   variability and uncertainties inherent in the existing climate models (Qing et al., 2020; Martel et al.,

707   2022), the projection findings under different scenarios were inconsistent, creating a challenge for pro-

708   active management and mitigation decisions. Despite the climate models' recognized flaws and

709   uncertainties, the general concordance between models and observations over many regions suggests

710   some improved confidence in their utility for understanding and mitigating future drought and climate

711   change (Cook et al., 2020). Furthermore, several reservoirs and a large number of wetlands are spread

712   throughout the NRB's tributaries (Meng et al., 2019), which individually and together play an essential

713   role in drought and flood risk reduction. We only investigated the impacts of mainstream reservoirs and

714   wetlands on drought and flood risk due to a lack of sub-basin reservoir operation observations. As a

715   result, future integrated wetland-reservoir simulations of all mainstream and tributaries for flood-

716   drought risk assessment will be done based on further data collection. Since the Nierji reservoir is the

717   largest in the NRB and has the most influence on the mainstream runoff regime, our findings based on

718   the simulation of Nierji reservoir and wetlands can give new insights into future floods and droughts, as

719   well as provide important support for future hydrological extremes adaptation.

720   4.2. The combining mitigation efficiency of wetlands and reservoir operation

721   The relative changes (compared with historical periods) of future flood and drought indices (Fig. 6

722   and 8), duration-peak flow-volume relationships (Fig. 7) and duration-deficit relationship (Fig. 9) differ

723   between the Nenjiang and Dalai stations under the same SSP scenario or in the same period, indicating

724   that reservoirs and downstream wetlands can modify the continuous propagation of upstream flood and

725   hydrological drought risks to the downstream. First, reservoirs and downstream wetlands can help to

726   reduce the risks of future floods and droughts to some extent, namely partially reduce flood peak flow

727   and flashiness, and decrease the number of droughts, annual drought days and drought deficit. Second,

728   reservoirs and downstream wetlands cannot completely eliminate flood and drought risks. Because the

729   flood duration and volume will overall increase at the Dalai station, especially that the extreme floods

730   will be more frequent in the future (Fig.7). Further, in addition to the number of droughts, the percentage

731   change values of the annual drought days, drought duration and deficit relative change at the Dalai

732   Station are greater than those of Nenjiang Station (Fig.8). This imply that the mitigation effects on

733   hydrological droughts is minimal. Such findings suggest that future climate change will lead to an

734   increase in the risk of hydrologic failure of existing reservoir and wetlands, thus posing large challenges

735   for future socio-and eco-hydrological systems in the downstream NRB.

736   Wetlands are typically viewed as green infrastructures and reservoirs are generally regarded as

737   important gray infrastructures. Although our study showed that the combining of reservoirs and

33

738   wetlands does not completely eliminate the risk of future hydrological extremes, they continue to play

739   an important role that cannot be ignored. The reservoir's inherent constraints are one factor contributing

740   to this likelihood of hydrological failure. This is because reservoirs only control floods and droughts

741   that occur downstream of them, limiting their effects to the regional scale (Brunner, 2021). The

742   regulation becomes less effective with distance increased due to "dilutions" effect caused by inflows

743   from downstream tributaries (Guo et al., 2012). Reservoirs cannot, however, play a considerable role in

744   basins where tributaries exist downstream, particularly those sub-basins prone to drought and flooding.

745   From these perspectives, widely distributed wetlands can provide a complementary and vital function

746   by providing biological function and hydrological regulation in regions where reservoirs are unable to

747   have an impact. On the other hand, the limited capacity of existing wetlands to regulate hydrology

748   increases the risk of hydrological failure to some extent. This is because, compared with the historical

749   period, the existing wetlands in the NRB have been seriously degraded, such as the weakening of the

750   connectivity between riparian wetlands and the river channel, and the increased fragmentation of

751   wetlands, among other changes (Chen et al., 2021). These degraded wetlands cannot play an effective

752   role in mitigating floods and droughts under future climate change.

753

754   4.3. Implications for flood and drought risk management under climate change

755   This modeling study predicts higher flood and drought risks in the NRB under the combined influence

756   of wetlands and reservoirs. This could impose a great challenge to the operation of the Nierji Reservoir

757   dam, i.e., to its effective operation for flood mitigation and drought alleviation. To curb the flood and

758   drought risks caused by future climate change in the NRB, it is urgent to improve the water regulation

759   capacity of the lower NRB. Although the Nierji Reservoir, as previously argued, plays an important role

760   in reducing floods and droughts, the potential for extreme hydrological events in the future necessitate

761   the application of various combinations of measures with different scales of implementation (i.e., hybrid

762   measures). We insist that the first remedial measure to be undertaken should be the implementation of

763   wetland restoration and protection projects, because studies have demonstrated that wetland coverage

764   and their spatial pattern can affect both basin physical conditions and human decision-making attitudes

765 toward risk (Gómez-Baggethun et al., 2019; Javaheri and Babbar-Sebens, 2014; Martinez-Martinez et

766 al., 2014; Zedler and Kercher, 2005). Given that the spatial location of wetlands within a river basin is

767 also important in determining the efficiency of their mitigation services (Gourevitch et al., 2020; Li et

768 al., 2021; Zhang and Song, 2014), optimization of wetland spatial patterns should be considered and can

769 be carried out to further enhance the role of wetlands in flood and drought defense.

770   In our view, the second important remedial measure that should be implemented is to improve the

771 existing reservoir operation schemes based on accurate hydrological forecasting. This requires, on one

772 hand, coupling of wetlands with hydrological processes and models to improve the simulation accuracy

773 of the upstream incoming water (i.e., runoff from the Nenjiang Station) to provide scientific support for

774 reservoir operation decisions. Concomitantly, it is necessary to modify the existing schemes for optimal

775 reservoir operation to improve the system's capacity to deal with extreme flood and drought risks.

776 Because the percentage increase in flood (Fig. 6) and drought indicators (Fig. 8) demonstrated that the

777 existing reservoir operation schemes are not effective in mitigating the risks associated with future

778 climate change-induced floods and droughts. Therefore, we need to re-examine and evaluate the flood

779 and drought risks in the NRB under future climate change and propose optimal operation schemes that

780 can maximize the reduction of flood and drought risks by the Nierji Reservoir. Traditionally, the water

781 level of a reservoir should be maintained at the designed flood limited water level during the flood

782 season, which does not consider river flow forecast. (Ding et al., 2015) analyzed a concept that provides

783 a dynamic control of the maximum allowed water level during the flood season, for the Nierji Reservoir

784 dam. A reasonable approach to tackle this issue could be to considerate forecast uncertainty and

785 acceptable flood risk to minimize the total loss caused by flood and drought. Further modeling studies

786 with multi-objective optimization algorithm can help identify an optimum reservoir operation for best

787 economic and ecological outcomes.

788 **5. Conclusions**

789   This study projected future flood and drought risks by considering the combined impacts of wetlands

790 and reservoirs. To achieve this, we developed a hydrological modeling framework coupled wetlands

791 and reservoir operations and then applied it in a case study involving a 297,000-km^2 large river basin in

792 northeast China. With this framework, we found that coupling wetlands and reservoir operations can

793 slightly increase model calibration results and efficiently improve model capacity to capture both flood

794 and hydrological drought characteristics in a river basin. The upper NRB will experience more severe

795 flood and hydrological droughts and can impose a great challenge to the effective operation of

796 downstream reservoir under the predicted future climate change scenarios. The risk of future floods and

797 hydrologic droughts along the lower NRB will further increase even under the combined influence of

798 reservoirs and wetlands. These results demonstrated that the risk of floods and droughts will overall

799 increase further under future climate change even under the combined influence of reservoirs and

800 wetlands, showing the urgency to implement wetland restoration and develop accurate forecasting

801 systems. To fully understand how wetland and reservoir operations may be influential and maintain an

802 acceptable level of risk, it is therefore necessary to consider an optimization of wetland spatial patterns

803 and reservoir operations simultaneously, thus achieving a collaborative optimization management to

804 maximum basin resilience to floods and hydrological droughts. Further, the effects of combining NBS

805 (e.g., wetlands) with traditional engineering solutions (e.g., reservoir) should both be useful and

806 necessary in the future for management decisions.

807

808 **Data Availability**

809 The data used in this study are openly available for research purposes. The five GCM outputs (GFDL-

810 ESM4, IPSL-CM6A-LR, MPI-ESM1-2-HR, MRI-ESM2-0, and UKESM1-0-L) used in this study are

811 publically available and were provided by the Inter-Sectoral Impact Model Intercomparison Project

812 (ISIMIP) (https://esg.pik-potsdam.de/search/isimip/). The CMhyd software is available at

813 https://swat.tamu.edu/software/cmhyd. The land-use/land-cover types, soil texture, and digital elevation

814 model for China can be downloaded from https://www.resdc.cn/. Data from the 88 weather stations

815 administered by National Meteorological Information Centre of China can be download at

816 http://data.cma.cn.

817

Author contribution

823

Competing interests

The authors declare that they have no known competing financial interests or personal relationships that could have appeared to influence the work reported in this paper.

827

Acknowledgments

833

834

Financial support

841   LAB94459).

842

843

844

845

846

847

848

849   **References**

850   Ahlén, I. et al., 2020. Wetlandscape size thresholds for ecosystem service delivery: Evidence from the

851   Norrström drainage basin, Sweden. Science of The Total Environment, 704: 135452.

852   Åhlén, I., Thorslund, J., Hambäck, P., Destouni, G. and Jarsjö, J., 2022. Wetland position in the landscape:

853   Impact on water storage and flood buffering. Ecohydrology, 15(7):e2458.

854   Alves, A., Gersonius, B., Kapelan, Z., Vojinovic, Z. and Sanchez, A., 2019. Assessing the Co-Benefits of

855   green-blue-grey infrastructure for sustainable urban flood risk management. Journal of Environmental

856   Management, 239: 244-254.

857   Anderson, C.C. and Renaud, F.G., 2021. A review of public acceptance of nature-based solutions: The

858   'why', 'when', and 'how' of success for disaster risk reduction measures. Ambio, 50(8): 1552-1573.

859   Arsenault, R., Brissette, F. and Martel, J., 2018. The hazards of split-sample validation in hydrological model

860   calibration. Journal of Hydrology, 566: 346-362.

861   Beven, K., 1981. Kinematic subsurface stormflow. Water Resources Research, 17(5): 1419-1424.

862   Bosshard, T., Kotlarski, S., Ewen, T. and Schär, C., 2011. Spectral representation of the annual cycle in the

863   climate change signal. Hydrology and Earth System Sciences, 15(9): 2777-2788.

864   Bouda, M. et al., 2014. Implementation of an automatic calibration procedure for HYDROTEL based on

865   prior OAT sensitivity and complementary identifiability analysis. Hydrological Processes, 28(12): 3947-

866   3961.

867   Bouda, M., Rousseau, A.N., Konan, B., Gagnon, P. and Gumiere, S.J., 2012. Bayesian Uncertainty Analysis

868   of the Distributed Hydrological Model HYDROTEL. Journal of Hydrologic Engineering, 17(9): 1021-1032.

869   Boulange, J., Hanasaki, N., Yamazaki, D. and Pokhrel, Y., 2021. Role of dams in reducing global flood

870   exposure under climate change. Nature Communications, 12(1).

871   Brunner, M.I., 2021. Reservoir regulation affects droughts and floods at local and regional scales.

872   Environmental Research Letters, 16(12): 124016.

873   Brunner, M.I., Slater, L., Tallaksen, L.M. and Clark, M., 2021. Challenges in modeling and predicting floods

874   and droughts: A review. WIREs Water, 8(3).

875   Cammalleri, C., Vogt, J. and Salamon, P., 2017. Development of an operational low-flow index for

876   hydrological drought monitoring over Europe. Hydrological sciences journal, 62(3): 346-358.

877   Casal-Campos, A., Fu, G., Butler, D. and Moore, A., 2015. An Integrated Environmental Assessment of

878   Green and Gray Infrastructure Strategies for Robust Decision Making. Environmental Science & Technology,

879   49(14): 8307-8314.

880   Chen, L., Wu, Y., Xu, Y.J. and Guangxin, Z., 2021. Alteration of flood pulses by damming the Nenjiang

881   River, China – Implication for the need to identify a hydrograph-based inundation threshold for protecting

882   floodplain wetlands. Ecological Indicators, 124: 107406.

883   Cheng, C., Brabec, E., Yang, Y. and Ryan, R., 2013. Rethinking stormwater management in a changing world:

884   Effects of detention for flooding hazard mitigation under climate change scenarios in the Charles River

885   Watershed, Proceedings of 2013 CELA Conference, Austin, Texas, pp. 27-30.

886   Chiang, F., Mazdiyasni, O. and AghaKouchak, A., 2021. Evidence of anthropogenic impacts on global

887   drought frequency, duration, and intensity. Nature Communications, 12(1).

888   Dang, T.D., Chowdhury, A.F.M.K. and Galelli, S., 2020. On the representation of water reservoir storage

889   and operations in large-scale hydrological models: implications on model parameterization and climate

890   change impact assessments. Hydrology and Earth System Sciences, 24(1): 397-416.

891   Diffenbaugh, N.S., Swain, D.L. and Touma, D., 2015. Anthropogenic warming has increased drought risk in

892   California. Proceedings of the National Academy of Sciences, 112(13): 3931-3936.

893   Ding, W. et al., 2015. An analytical framework for flood water conservation considering forecast uncertainty

894   and acceptable risk. Water Resources Research, 51(6): 4702-4726.

895   Dobson, B., Wagener, T. and Pianosi, F., 2019. An argument-driven classification and comparison of

896   reservoir operation optimization methods. Advances in Water Resources, 128: 74-86.

897   Eriyagama, N., Smakhtin, V. and Udamulla, L., 2020. How much artificial surface storage is acceptable in a

898   river basin and where should it be located: A review. Earth-Science Reviews, 208: 103294.

899   Evenson, G.R. et al., 2018. A watershed-scale model for depressional wetland-rich landscapes. Journal of

900   Hydrology X, 1: 100002.

901   Evenson, G.R., Golden, H.E., Lane, C.R. and D Amico, E., 2015. Geographically isolated wetlands and

902   watershed hydrology: A modified model analysis. Journal of Hydrology, 529: 240-256.

903   Evenson, G.R., Golden, H.E., Lane, C.R. and D'Amico, E., 2016. An improved representation of

904   geographically isolated wetlands in a watershed-scale hydrologic model. Hydrological Processes, 30(22):

905   4168-4184.

906   Fleig, A.K., Tallaksen, L.M., Hisdal, H. and Demuth, S., 2006. A global evaluation of streamflow drought

907   characteristics. Hydrol. Earth Syst. Sci., 10(4): 535-552.

908   Fortin, J. et al., 2001. Distributed Watershed Model Compatible with Remote Sensing and GIS Data. I:

909   Description of Model. Journal of Hydrologic Engineering, 6(2): 91-99.

910   Fossey, M., Rousseau, A.N., Bensalma, F., Savary, S. and Royer, A., 2015a. Integrating isolated and riparian

911   wetland modules in the PHYSITEL/HYDROTEL modelling platform: model performance and diagnosis.

912   Hydrological Processes, 29(22): 4683-4702.

913   Fossey, M., Rousseau, A.N., Bensalma, F., Savary, S. and Royer, A., 2015b. Integrating isolated and riparian

914   wetland modules in the PHYSITEL/HYDROTEL modelling platform: model performance and diagnosis.

915   Hydrological Processes, 29(22): 4683-4702.

916   Foulon, É., Rousseau, A.N. and Gagnon, P., 2018. Development of a methodology to assess future trends in

917   low flows at the watershed scale using solely climate data. Journal of Hydrology, 557: 774-790.

918   Fowler, K., Peel, M., Western, A. and Zhang, L., 2018. Improved Rainfall‑Runoff Calibration for Drying

919   Climate: Choice of Objective Function. Water Resources Research, 54(5): 3392-3408.

920   Garcia, F., Folton, N. and Oudin, L., 2017. Which objective function to calibrate rainfall‑runoff models for

921   low-flow index simulations? Hydrological Sciences Journal, 62(7): 1149-1166.

922   Golden, H.E., Lane, C.R., Rajib, A. and Wu, Q., 2021. Improving global flood and drought predictions:

923   integrating non-floodplain wetlands into watershed hydrologic models. Environmental Research Letters,

924   16(9): 091002.

925   Gómez-Baggethun, E. et al., 2019. Changes in ecosystem services from wetland loss and restoration: An

926   ecosystem assessment of the Danube Delta (1960 – 2010). Ecosystem Services, 39: 100965.

927   Gourevitch, J.D. et al., 2020. Spatial targeting of floodplain restoration to equitably mitigate flood risk.

928   Global Environmental Change, 61: 102050.

929   Gulbin, S., Kirilenko, A.P., Kharel, G. and Zhang, X., 2019. Wetland loss impact on long term flood risks in

930   a closed watershed. Environmental Science & Policy, 94: 112-122.

931   Güneralp, B., Güneralp, 0. and Liu, Y., 2015. Changing global patterns of urban exposure to flood and

932   drought hazards. Global Environmental Change, 31: 217-225.

933   Guo, H., Hu, Q., Zhang, Q. and Feng, S., 2012. Effects of the Three Gorges Dam on Yangtze River flow and

934   river interaction with Poyang Lake, China: 2003-2008. Journal of Hydrology, 416: 19-27.

935   Gupta, H.V., Kling, H., Yilmaz, K.K. and Martinez, G.F., 2009. Decomposition of the mean squared error

936   and NSE performance criteria: Implications for improving hydrological modelling. Journal of Hydrology,

937   377(1-2): 80-91.

938   Hagemann, S. and Jacob, D., 2007. Gradient in the climate change signal of European discharge predicted

939   by a multi-model ensemble. Climatic Change, 81(S1): 309-327.

940   Hallegatte, S., Green, C., Nicholls, R.J. and Corfee-Morlot, J., 2013. Future flood losses in major coastal

941   cities. Nature climate change, 3(9): 802-806.

942   Hirabayashi, Y. et al., 2013. Global flood risk under climate change. Nature Climate Change, 3(9): 816-821.

943   Hisdal, H. and Tallaksen, L.M., 2003. Estimation of regional meteorological and hydrological drought

944   characteristics: a case study for Denmark. Journal of Hydrology, 281(3): 230-247.

945   Hutchinson, M.F. and Xu, T., 2004. Anusplin version 4.2 user guide. Centre for Resource and Environmental

946   Studies. The Australian National University. Canberra, 5.

947   Javaheri, A. and Babbar-Sebens, M., 2014. On comparison of peak flow reductions, flood inundation maps,

948   and velocity maps in evaluating effects of restored wetlands on channel flooding. Ecological Engineering,

949   73: 132-145.

950   Jongman, B., 2018. Effective adaptation to rising flood risk. Nature Communications, 9(1): 1986.

951   Kharrufa, N.S., 1985. Simplified equation for evapotranspiration in arid regions. Hydrologie Sonderheft, 5(1):

952   39 – 47.

953   Kriegler, E. et al., 2017. Fossil-fueled development (SSP5): An energy and resource intensive scenario for

954   the 21st century. Global Environmental Change, 42: 297-315.

955   Kumar, P. et al., 2021. Nature-based solutions efficiency evaluation against natural hazards: Modelling

956   methods, advantages and limitations. Sci Total Environ, 784: 147058.

957   Lee, S. et al., 2018. Assessing the cumulative impacts of geographically isolated wetlands on watershed

958   hydrology using the SWAT model coupled with improved wetland modules. Journal of Environmental

959   Management, 223: 37-48.

960   Liu, D., 2020. A rational performance criterion for hydrological model. Journal of Hydrology, 590: 125488.

961   https://doi.org/10.1016/j.jhydrol.2020.125488.

962   Li, F., Zhang, G. and Xu, Y.J., 2014. Spatiotemporal variability of climate and streamflow in the Songhua

963   River Basin, northeast China. Journal of Hydrology, 514: 53-64.

964   Li, W. et al., 2021. Where and how to restore wetland by utilizing storm water at the regional scale: A case

965   study of Fangshan, China. Ecological Indicators, 122: 107246.

966   Lobligeois, F., Andréassian, V., Perrin, C., Tabary, P. and Loumagne, C., 2014. When does higher spatial

967   resolution rainfall information improve streamflow simulation? An evaluation using 3620 flood events.

968   Hydrology and Earth System Sciences, 18(2): 575-594.

969   Maes, J. et al., 2015. More green infrastructure is required to maintain ecosystem services under current

970   trends in land-use change in Europe. Landscape Ecology, 30(3): 517-534.

971   Manfreda, S., Miglino, D. and Albertini, C., 2021. Impact of detention dams on the probability distribution

972   of floods. Hydrology and Earth System Sciences, 25(7): 4231-4242.

973   Maraun, D., 2016. Bias Correcting Climate Change Simulations - a Critical Review. Current Climate Change

974   Reports, 2(4): 211-220.

975   Martinez-Martinez, E., Nejadhashemi, A.P., Woznicki, S.A. and Love, B.J., 2014. Modeling the hydrological

976   significance of wetland restoration scenarios. Journal of Environmental Management, 133: 121-134.

977   Melsen, L.A. et al., 2019. Subjective modeling decisions can significantly impact the simulation of flood and

978   drought events. Journal of Hydrology, 568: 1093-1104.

979   Meng, B., Liu, J., Bao, K. and Sun, B., 2019. Water fluxes of Nenjiang River Basin with ecological network

980   analysis: Conflict and coordination between agricultural development and wetland restoration. Journal of

981   Cleaner Production, 213: 933-943.

982   Moore, K., Pierson, D., Pettersson, K., Schneiderman, E. and Samuelsson, P., 2008. Effects of warmer world

983   scenarios on hydrologic inputs to Lake Mälaren, Sweden and implications for nutrient loads. Hydrobiologia,

984   599(1): 191-199.

985   Moriasi, D.N., 2007. Model Evaluation Guidelines for Systematic Quantification of Accuracy in Watershed

986   Simulations. Transactions of the ASABE, 50(3): 885-900.

987   Moriasi, D.N., Gitau, M.W., Pai, N. and Daggupati, P., 2015. Hydrologic and water quality models:

988   Performance measures and evaluation criteria. Transactions of the ASABE, 58(6): 1763-1785.

989   Moriasi, D.N., Gitau, M.W., Pai, N. and Daggupati, P., 2015. Hydrologic and water quality models:

990   Performance measures and evaluation criteria. Transactions of the ASABE, 58(6): 1763-1785.

991   Muller, M., 2019. Hydropower dams can help mitigate the global warming impact of wetlands. Nature,

992   566(7744): 315-317.

993   N. Moriasi, D. et al., 2007. Model Evaluation Guidelines for Systematic Quantification of Accuracy in

994   Watershed Simulations. Transactions of the ASABE, 50(3): 885-900.

995   Nash, J.E. and Sutcliffe, J.V., 1970. River flow forecasting through conceptual models part I—A discussion

996   of principles. Journal of hydrology, 10(3): 282-290.

997   Nelson, D.R., Bledsoe, B.P., Ferreira, S. and Nibbelink, N.P., 2020. Challenges to realizing the potential of

998   nature-based solutions. Current Opinion in Environmental Sustainability, 45: 49-55.

999   Nika, C.E. et al., 2020. Nature-based solutions as enablers of circularity in water systems: A review on

1000   assessment methodologies, tools and indicators. Water Research, 183: 115988.

1001   Noël, P., Rousseau, A.N., Paniconi, C. and Nadeau, D.F., 2014. Algorithm for delineating and extracting

1002   hillslopes and hillslope width functions from gridded elevation data. Journal of Hydrologic Engineering,

1003   19(2): 366-374.

1004   O'Neill, B.C. et al., 2016. The Scenario Model Intercomparison Project (ScenarioMIP) for CMIP6.

1005   Geoscientific Model Development, 9(9): 3461-3482.

1006   Park, J., Botter, G., Jawitz, J.W. and Rao, P.S.C., 2014. Stochastic modeling of hydrologic variability of

1007   geographically isolated wetlands: Effects of hydro-climatic forcing and wetland bathymetry. Advances in

1008   Water Resources, 69: 38-48.

1009   Pool, S., Vis, M., Seibert, J. and Sveriges, L., 2018. Evaluating model performance: towards a non-parametric

1010   variant of the Kling-Gupta efficiency. Hydrological sciences journal, 63(13-14): 1941-1953.

1011   Rajib, A., Golden, H.E., Lane, C.R. and Wu, Q., 2020. Surface Depression and Wetland Water Storage

1012   Improves Major River Basin Hydrologic Predictions. Water Resources Research, 56(7): e2019WR026561.

1013   Rousseau, A.N. et al., 2011. PHYSITEL, a specialized GIS for supporting the implementation of distributed

1014   hydrological models. Water News-Official Magazine of the Canadian Water Resources Association, 31(1):

1015   18-20.

1016   Saharia, M. et al., 2017. Mapping Flash Flood Severity in the United States. Journal of Hydrometeorology,

1017   18(2): 397-411.

1018   Schneider, C., Flörke, M., De Stefano, L. and Petersen-Perlman, J.D., 2017. Hydrological threats to riparian

1019   wetlands of international importance – a global quantitative and qualitative analysis. Hydrology and Earth

1020   System Sciences, 21(6): 2799-2815.

1021   Seibert, J., Vis, M.J.P., Lewis, E. and Meerveld, H.J., 2018. Upper and lower benchmarks in hydrological

1022   modelling. Hydrological Processes, 32: 1120 - 1125.

1023   Shafeeque, M. and Luo, Y., 2021. A multi-perspective approach for selecting CMIP6 scenarios to project

1024   climate change impacts on glacio-hydrology with a case study in Upper Indus river basin. Journal of

1025   Hydrology, 599: 126466.

1026   Shook, K., Papalexiou, S. and Pomeroy, J.W., 2021. Quantifying the effects of Prairie depressional storage

1027   complexes on drainage basin connectivity. Journal of Hydrology, 593: 125846.

1028   Smakhtin, V.U., 2001. Low flow hydrology: a review. Journal of Hydrology, 240(3): 147-186.

1029   Staudinger, M., Stahl, K., Seibert, J., Clark, M.P. and Tallaksen, L.M., 2011. Comparison of hydrological

1030   model structures based on recession and low flow simulations. Hydrology and Earth System Sciences, 15(11):

1031   3447-3459.

1032   Tallaksen, L.M. and van Lanen, H.A.J., 2004. Hydrological drought; processes and estimation methods for

1033   streamflow and groundwater. Developments in water science, 48.

1034   Thorslund, J. et al., 2017. Wetlands as large-scale nature-based solutions: Status and challenges for research,

1035   engineering and management. Ecological Engineering, 108: 489-497.

1036   Tolson, B.A. and Shoemaker, C.A., 2007. Dynamically dimensioned search algorithm for computationally

1037   efficient watershed model calibration. Water Resources Research, 43(1): 1-6.

1038   Turcotte, R., Fortin, L.G., Fortin, V., Fortin, J.P. and Villeneuve, J.P., 2007. Operational analysis of the

1039   spatial distribution and the temporal evolution of the snowpack water equivalent in southern Québec, Canada.

1040   Hydrology Research, 38(3): 211-234.

1041   UNISDR, C., 2015. The human cost of natural disasters: A global perspective.

1042   van Vuuren, D.P. et al., 2017. The Shared Socio-economic Pathways: Trajectories for human development

1043   and global environmental change. Global Environmental Change, 42: 148-152.

1044   Walz, Y. et al., 2021. Disaster-related losses of ecosystems and their services. Why and how do losses matter

1045   for disaster risk reduction? International Journal of Disaster Risk Reduction, 63: 102425.

1046   Wang, L., Chen, X., Shao, Q. and Li, Y., 2015. Flood indicators and their clustering features in Wujiang

1047   River, South China. Ecological Engineering, 76: 66-74.

1048   Wang, S., Zhang, L., She, D., Wang, G. and Zhang, Q., 2021. Future projections of flooding characteristics

1049   in the Lancang-Mekong River Basin under climate change. Journal of Hydrology, 602: 126778.

1050   Wang, X., Yang, W. and Melesse, A.M., 2008. Using Hydrologic Equivalent Wetland Concept Within

1051   SWAT to Estimate Streamflow in Watersheds with Numerous Wetlands. Transactions of the ASABE, 51(1):

1052   55-72.

1053   Ward, P.J. et al., 2020. The need to integrate flood and drought disaster risk reduction strategies. Water

1054   Security, 11: 100070.

1055   Wu, Y., Zhang, G., Rousseau, A.N. and Xu, Y.J., 2020. Quantifying streamflow regulation services of

1056   wetlands with an emphasis on quickflow and baseflow responses in the Upper Nenjiang River Basin,

1057   Northeast China. Journal of Hydrology, 583: 124565.

1058   Wu, Y., Zhang, G., Rousseau, A.N., Xu, Y.J. and Foulon, É., 2020. On how wetlands can provide flood

1059   resilience in a large river basin: A case study in Nenjiang river Basin, China. Journal of Hydrology, 587:

1060   125012.

1061   Wu, Y., Zhang, G., Xu, Y.J. and Rousseau, A.N., 2021. River Damming Reduces Wetland Function in

1062   Regulating Flow. Journal of Water Resources Planning and Management, 147(10).

1063   Xu, X. et al., 2019. Evaluating the impact of climate change on fluvial flood risk in a mixed-use watershed.

1064   Environmental Modelling & Software, 122: 104031.

1065 Yassin, F. et al., 2019. Representation and improved parameterization of reservoir operation in hydrological

1066 and land-surface models. Hydrology and Earth System Sciences, 23(9): 3735-3764.

1067 Zedler, J.B. and Kercher, S., 2005. WETLAND RESOURCES: Status, Trends, Ecosystem Services, and

1068 Restorability. Annual Review of Environment and Resources, 30(1): 39-74.

1069 Zelenhasić, E. and Salvai, A., 1987. A method of streamflow drought analysis. Water resources research,

1070 23(1): 156-168.

1071 Zeng, L., Shao, J. and Chu, X., 2020. Improved hydrologic modeling for depression-dominated areas. Journal

1072 of Hydrology, 590: 125269.

1073 Zhang, X. and Song, Y., 2014. Optimization of wetland restoration siting and zoning in flood retention areas

1074 of river basins in China: A case study in Mengwa, Huaihe River Basin. Journal of Hydrology, 519: 80-93.

1075 Zhao, G., Gao, H., Naz, B.S., Kao, S. and Voisin, N., 2016. Integrating a reservoir regulation scheme into a

1076 spatially distributed hydrological model. Advances in Water Resources, 98: 16-31.

1077 Zhao, Y. et al., 2021. Future precipitation, hydrology and hydropower generation in the Yalong River Basin:

1078 Projections and analysis. Journal of Hydrology, 602: 126738.

1079